DOE/NV/03624--0878

LLNL-TR-813599

GEOLOGIC FRAMEWORK MODEL FOR THE DRY ALLUVIUM GEOLOGY (DAG) EXPERIMENT TESTBED YUCCA FLAT, NEVADA NATIONAL SECURITY SITE

Prepared for:

U.S. Department of Energy
National Nuclear Security Administration
National Center for Nuclear Security

Prepared by:

Lance Prothro
Geoscience Operations, Mission Support and Test Services, LLC
Mercury, Nevada

And

Jeffrey Wagoner, Lawrence Livermore National Laboratory

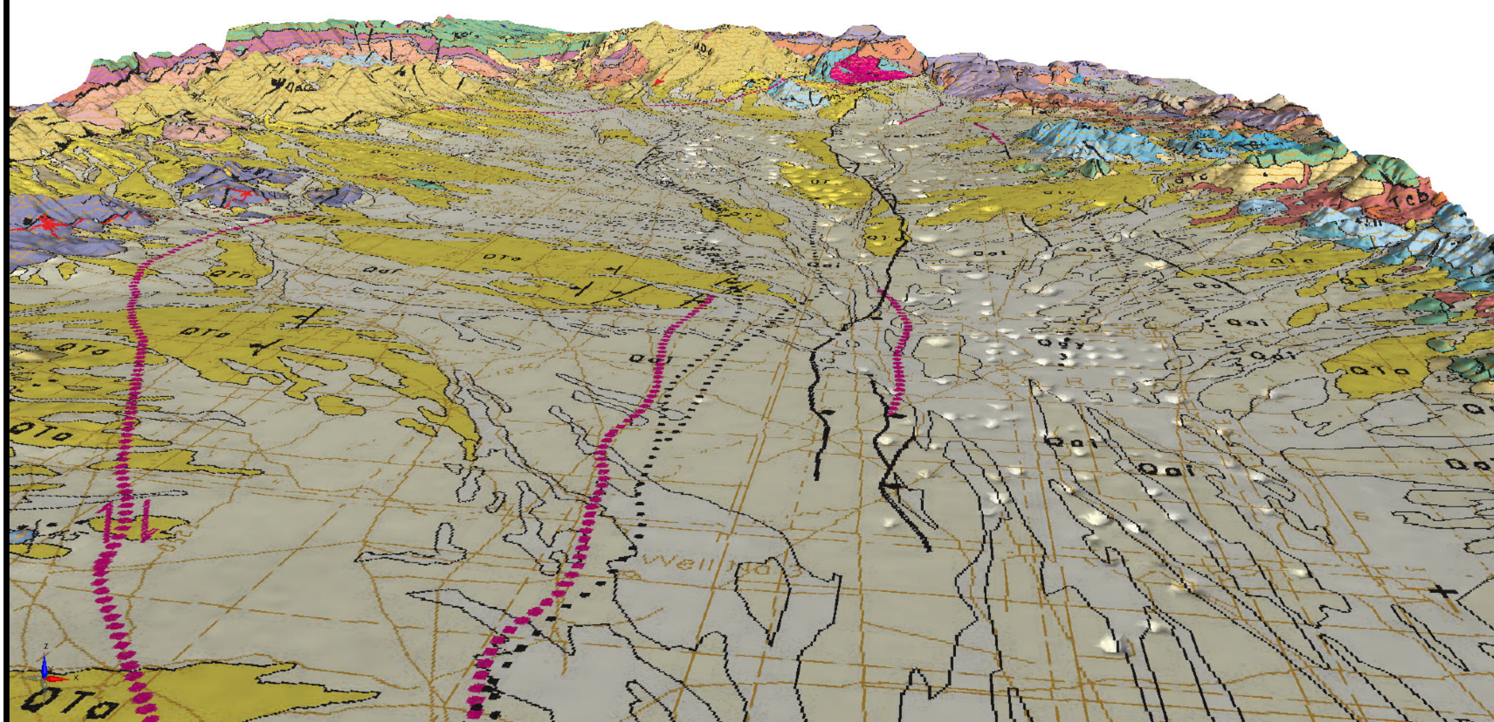

September 2020

DISCLAIMER STATEMENT

This work was performed under the auspices of the U.S. Department of Energy's National Nuclear Security Administration by Mission Support and Test Services, LLC under Contract No. DE-NA0003624 with the U.S. Department of Energy. This report describes objective technical results and analysis. Any subjective views or opinions that might be expressed in the report do not necessarily represent the views of the U.S. Department of Energy or the United States Government:

This work performed under the auspices of the U.S. Department of Energy by Lawrence Livermore National Laboratory under Contract DE-AC52-07NA27344.

DOE/NV/03624--0878

LLNL-TR-813599

Geologic Framework Model for the Dry Alluvium Geology (DAG) Experiment Testbed Yucca Flat, Nevada National Security Site

Prepared by:

Lance Prothro
Geoscience Operations
Mission Support and Test Services, LLC

And
Jeffrey Wagoner
Lawrence Livermore National Laboratory

September 2020

This page intentionally left blank.

Executive Summary

Geologic framework models (GFMs) provide a methodology for integrating geology into, and thus geologically informing, other modeling and simulation activities. GFMs provide a three-dimensional (3-D), geology-based digital framework for developing and parametrizing meshes and evaluating model and simulation results. This report describes a 3-D GFM constructed for the Source Physics Experiment Phase II Dry Alluvium Geology test series located in Yucca Flat at the Nevada National Security Site. The geology in the Yucca Flat region is complex and diverse, which creates challenges to modeling seismic wave propagation from SPE tests. The Yucca Flat GFM helps address these challenges by providing the 3-D distribution of relevant geologic features and physical properties necessary to more effectively model seismic wave propagation. The GFM includes 7 model layers and 48 faults that cut and offset the layers. An appendix is included that provides quantitative data on physical properties for each model layer.

Table of Contents

List of Appendices

List of Figures

List of Tables

List of Acronyms and Abbreviations

2-D	two-dimensional
3-D	three-dimensional
AL	alluvium
BN	Bechtel Nevada
DAG	Dry Alluvium Geology (Experiment)
ft	feet (foot)
GFM	geologic framework model
HFM	hydrostratigraphic framework model
LWT	lower welded tuff
m	meter(s)
ma	million years ago
MZ	Mesozoic granitic rocks
PZ	Paleozoic rocks
QC	quality check
SPE	Source Physics Experiment
UGTA	Underground Test Area
UWT	upper welded tuff
VNT	vitric nonwelded tuff
WTP	Weapons Testing Program
ZNT	zeolitic nonwelded tuff

Geologic Framework Model for the Dry Alluvium Geology (DAG) Experiment Testbed, Yucca Flat, Nevada National Security Site

July 2020

1.0 Introduction

Geologic framework models (GFMs) provide a methodology for integrating geology into, and thus geologically informing, other modeling and simulation activities. GFMs provide a three-dimensional (3-D) geology-based digital framework for developing and parametrizing meshes and evaluating model and simulation results. This report describes a 3-D GFM constructed for the Source Physics Experiment (SPE) Phase II Dry Alluvium Geology (DAG) test series located in Yucca Flat (Figure 1). The geology in the Yucca Flat region is complex and diverse, which creates challenges to modeling seismic wave propagation from SPE tests. The DAG Yucca Flat GFM helps address these challenges by providing the 3-D distribution of relevant geologic features and physical properties necessary to more effectively model seismic wave propagation. The GFM includes 7 model layers and 48 faults that cut and offset the layers (Figure 2).

2.0 Geologic Setting

Yucca Flat is a north-south-elongated elliptical-shaped valley in the northeastern portion of the Nevada National Security Site (NNSS). It extends approximately 30 kilometers (km) north-south and 18 km east-west. It is a closed topographic, alluvium-filled basin. Surface drainage from the surrounding highlands is towards the center and southern portions of the basin and culminates in a playa (seasonally dry lake) at the southern end of the valley (Figure 3).

Rocks in the vicinity of Yucca Flat range in age from approximately 750 million years old to recent sediments deposited in active washes (Slate et al. 1999). The rocks can be grouped into five general categories (Figure 3). From oldest to youngest, these are: Late Precambrian and Paleozoic sedimentary rocks (~750 – ~280 millions of years ago [Ma]), Mesozoic granite (~100 Ma), Tertiary volcanic rocks (~15 – 11.45 Ma), Tertiary to Quaternary alluvial deposits (~10 Ma to recent), and Quaternary playa deposits (0.01 Ma to recent).

Late Precambrian rocks outcrop in isolated exposures in the northeastern and extreme northwestern portions of the model area, and consist mainly of quartzite, shale, and conglomerate (Cole et al. 1997). These rocks are approximately 2,500 meters (m) thick in the NNSS region.

The overlying Paleozoic rocks consist mainly of limestone and dolomite except in the upper portion where quartzite, shale, and conglomerate dominate the stratigraphic section. The Paleozoic carbonate rocks outcrop in the highlands bordering Yucca Flat on the east and southwest, and to a lesser extent in the highlands north of Yucca Flat. These rocks also compose the “basement” beneath most of Yucca Flat (Cole et al. 1997). The upper Paleozoic siliciclastic rocks dominate the highlands along the northwestern margin of Yucca Flat. Total thickness of the Paleozoic section at the NNSS is approximately 8,000 m.

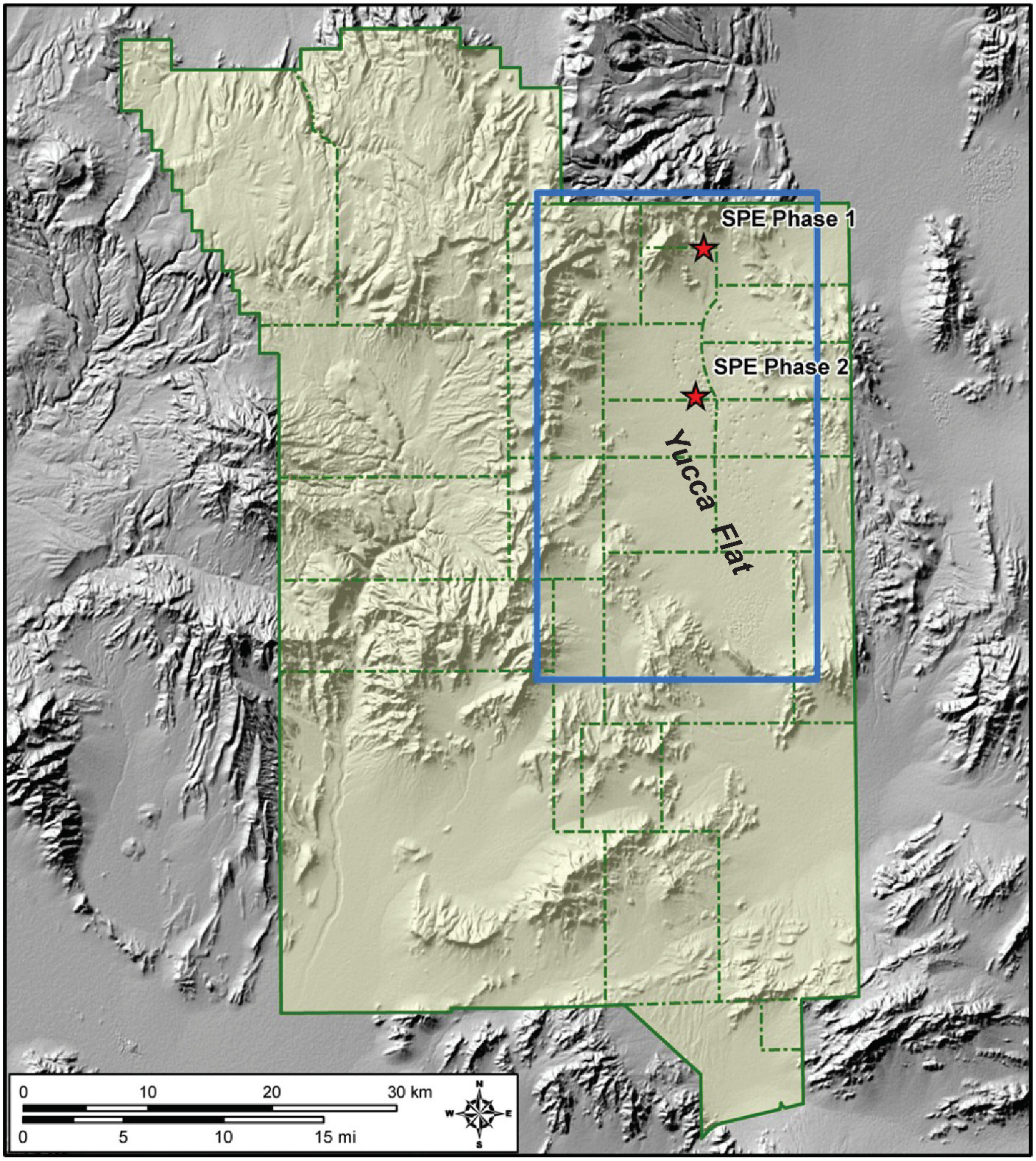

Figure 1
Shaded Relief Map of the NNSS Showing Location of the DAG Yucca Flat GFM (blue rectangle)

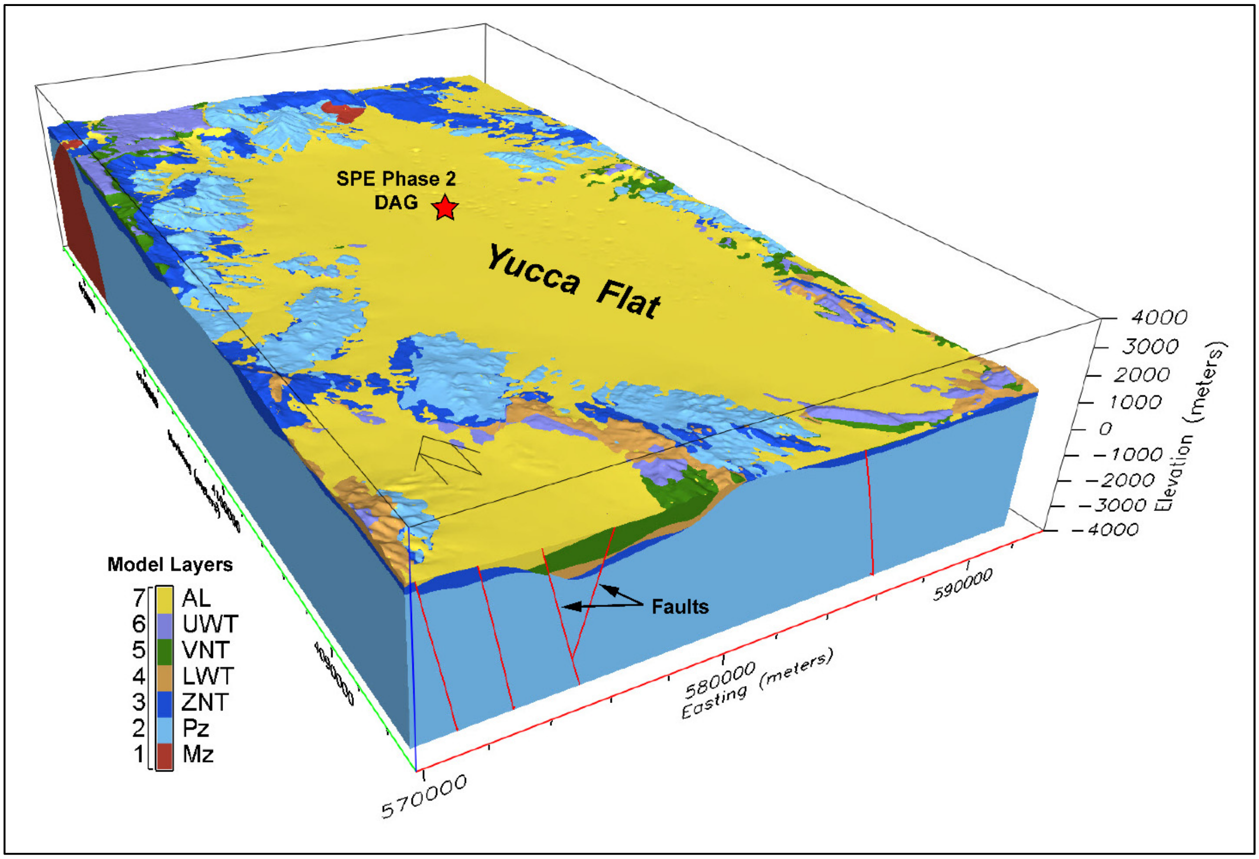

Figure 2
3-D Perspective View of the DAG Yucca Flat GFM Looking Northeast

Legend:

AL = Alluvium
UWT = Upper welded tuff
VNT = Vitric nonwelded tuff
LWT = Lower welded tuff
ZNT = Zeolitic nonwelded tuff
PZ = Paleozoic rocks
MZ = Mesozoic granitic rocks

See Table 4 and Appendix A for additional information

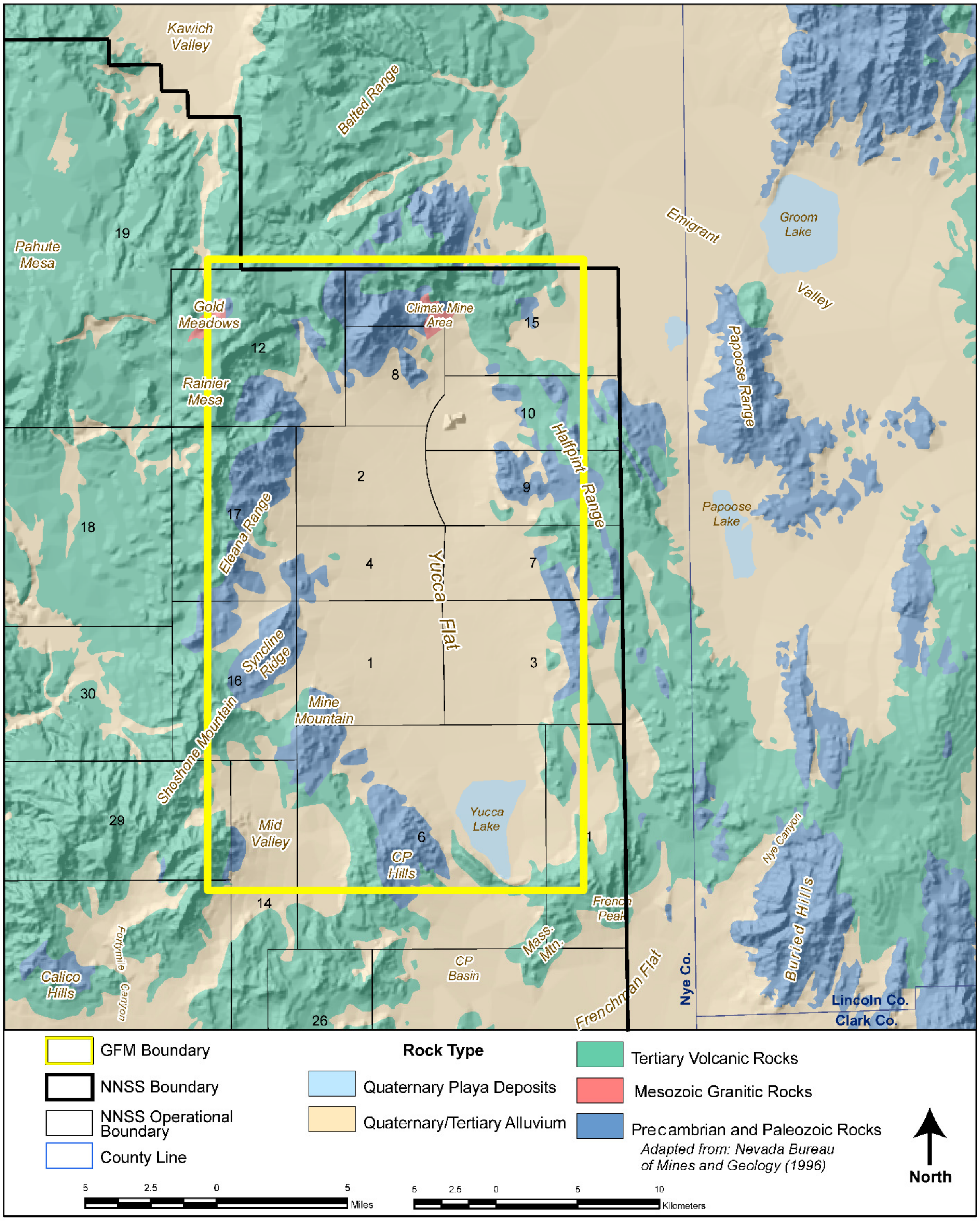

Figure 3
Generalized Geologic Map of the DAG Yucca Flat GFM Area

The Precambrian and Paleozoic rocks were deformed by compressional forces sometime between approximately 250 and 100 Ma (Cole and Cashman 1999). Regionally, this deformation resulted in eastward-directed folding and thrust faulting associated with the Belted Range thrust fault system located in the far northwestern portion of the model area (Figure 4). Beneath the western portion of Yucca Flat, however, compressional deformation is directed westward, and is associated with the slightly younger CP thrust fault, a local back thrust, which places Paleozoic carbonate rocks over younger upper Paleozoic siliciclastic rocks. In general, compressional deformation is more intense in the western portion of the model area.

Following compressional deformation, the Precambrian and Paleozoic rocks were intruded by granitic magma 100 Ma in two main places in the far northern portion of the model area (Slate et al. 1999). The resulting Cretaceous granitic rocks are now exposed at the Climax stock at the north end of Yucca Flat and the Gold Meadows stock west of Rainier Mesa in the far northwestern portion of the model area. The stocks are compositionally very similar, consisting of quartz monzonite and granodiorite. Geophysical data indicate that the two stocks are steep-sided cupolas that rise up approximately 4,000 m from a larger single intrusion (Phelps et al. 2004).

Tertiary volcanic rocks unconformably overlie the older sedimentary and granitic rocks in many places around the margins and beneath Yucca Flat. These volcanic rocks are generally rhyolitic in composition and consist of ash-flow, ash- and pumice-fall, and reworked tuffs erupted between approximately 15 to 11 Ma from large volcanos and associated vents located west and northwest of Yucca Flat (Sawyer et al. 1994).

The Yucca Flat alluvial basin began forming approximately 10 Ma as a result of generally east-west-directed basin-and-range extension (Cole et al. 1997). This resulted in eroded debris from the developing highlands being shed into the structurally subsiding Yucca Flat basin. This alluvial debris, which now fills the basin, is more than 900 m thick in the southern portion of Yucca Flat. The alluvium generally consists of mixtures of silt, sand, and gravel deposited by alluvial fan processes. At the lowest elevations in the southern portions of Yucca Flat where gradients approach zero, finer-grained silt and clay sediments have been deposited, forming playa deposits. Figure 5 provides a more detailed depiction of the rock section in the Yucca Fat region and shows how the seven model layers of the DAG Yucca Flat GFM correlate with the various rock units.

Faulting and associated basin development in Yucca Flat is accommodated mainly along generally north-striking down-to-the-east normal faults (Cole et al. 1997). The vast majority of the faults are buried, and thus do not have surface expression, and are only known from geophysical surveys and drilling. Notable exceptions include the Yucca Fault, which has a conspicuous eroded scarp that runs more than 20 km through the center of Yucca Flat, and is interpreted to have had movement with surface rupture within the last 138,000 years (U.S. Geological Survey 2006). Numerous surface cracks, fissures, and small scarps formed along the Yucca Fault surface scarp during nearby underground nuclear testing (Grasso 2001). The Carpetbag Fault in the northwest portion of Yucca Flat ruptured the surface after the nearby CARPETBAG underground nuclear test in 1970 (Jenkins 1973). Prior to 1970, the fault was only suspected based on surface lineaments observed on aerial photographs and gravity data.

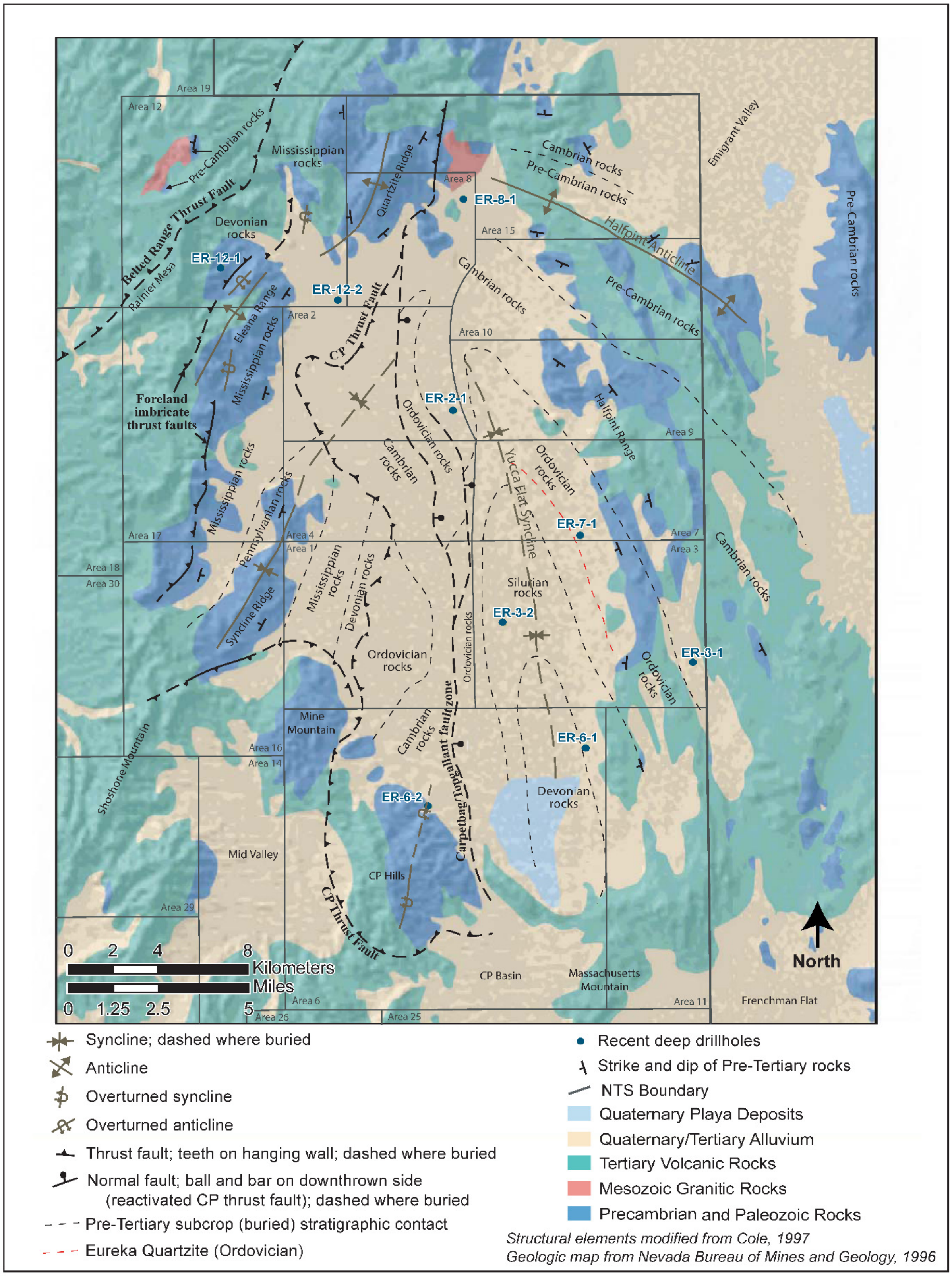

Figure 4
Pre-Tertiary Structure of the Yucca Flat Area

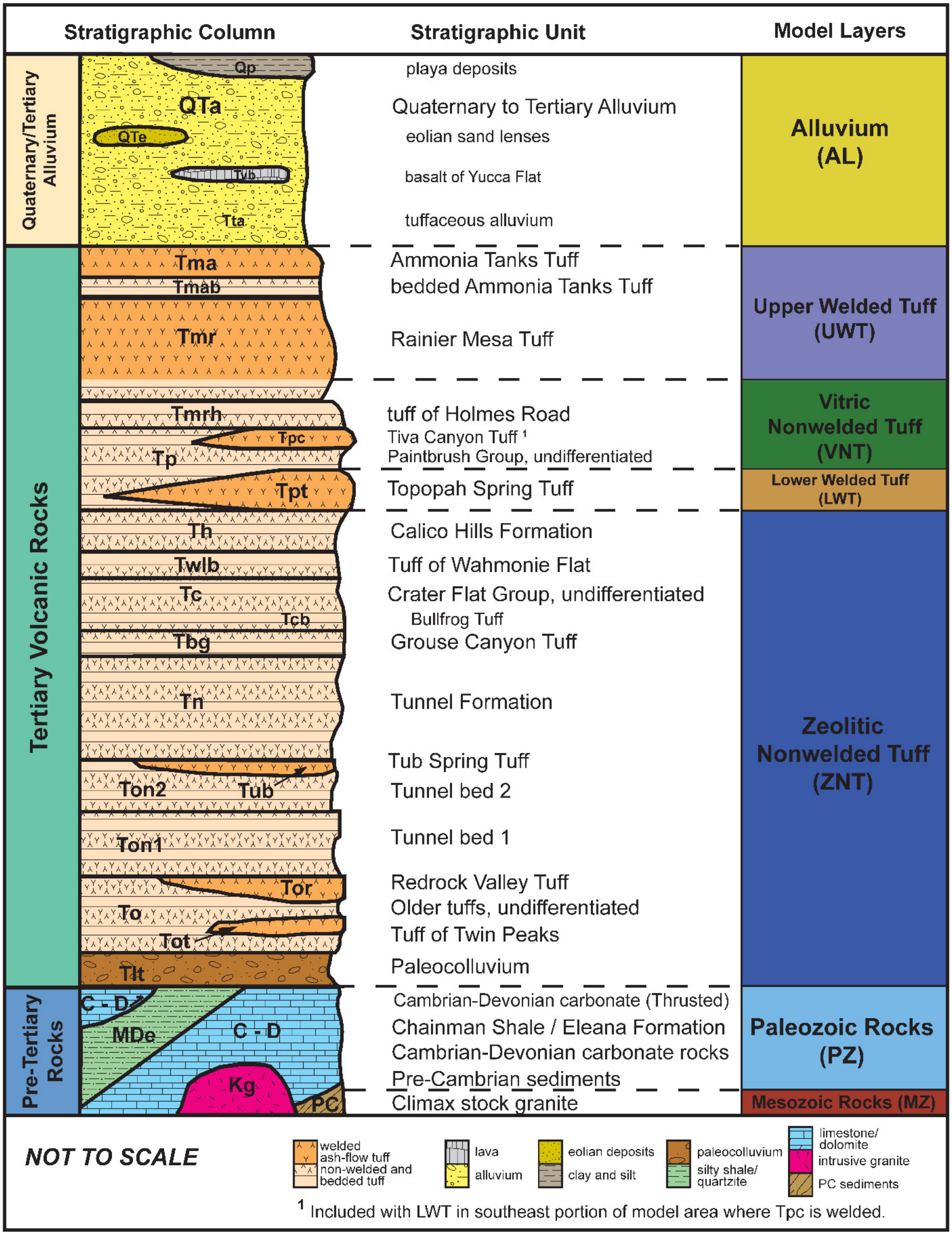

Figure 5
Stratigraphic Column of the Yucca Flat Region

Surface rupture of the Carpetbag Fault produced several fault scarps, with the western scarp being 2,500 m long and having up to 5.9 m of down-on-the-east dip-slip displacement (Garcia and Sharps 1985).

Structurally, Yucca Flat consists of two basins, a larger and deeper main basin that includes most of the eastern half of Yucca Flat, and a smaller and shallower western sub-basin (Figure 6). The two basins are separated by a prominent north-south-trending buried ridge of Paleozoic carbonate rocks. The buried ridge is clearly observed in the gravity data and has been confirmed by drilling. Geologic and geophysical log data from drill holes indicate volcanic rocks are absent in places along the top of the ridge, resulting in alluvium lying directly on Paleozoic carbonate rocks. The alluvium is also quite thin in places along the ridge. At the Gravity High 1 borehole in Area 2, 44 m of alluvium was observed overlying Paleozoic dolomite. Southward along the buried ridge in Area 1, drill hole TG2 (also referred to as Gravity High 2) penetrated only 22 m of alluvium before encountering Paleozoic carbonate.

The main Yucca Flat basin is a highly faulted, west-tilted half-graben bound on the west by the buried ridge and large east-dipping basin-forming normal faults associated with the north-trending Carpetbag/Topgallant fault system (Cole et al. 1997). Offset along the Carpetbag/Topgallant fault system exceeds 1,300 m in places. The Yucca Fault, mentioned above and located east of the Carpetbag/Topgallant fault system, is also a major fault within the main Yucca Flat basin with down-to-the-east offset that exceeds 300 m. The smaller and shallower western sub-basin resembles more of a full graben bounded by east- and west-dipping normal faults that have offsets considerably less than those of the Carpetbag/Topgallant fault system.

3.0 Methodology

The DAG Yucca Flat GFM integrates data, concepts, and components from two pre-existing GFMs. A legacy 4-layer GFM was constructed starting in the mid-1990s and is the basis for modeling seismic wave simulations from SPE Phase 1 experiments located at the north end of Yucca Flat (Wagoner 2014). For the SPE Phase 2 DAG series, the SPE Phase I GFM was "merged" with an existing, more detailed GFM developed for groundwater flow and contaminant transport modeling (Bechtel Nevada [BN] 2006) to increase model detail within the Yucca Flat basin where DAG is located. This required constructing a new separate GFM using various data and components from the existing GFMs, as described in the following subsections.

3.1 Model Construction

The DAG Yucca Flat GFM was constructed using EarthVision Version 10 by Dynamic Graphics, Inc. (http://www.dgi.com/earthvision/evmain.html). EarthVision is a powerful software platform for 3-D geologic model building, analysis, and visualization. Construction of the DAG Yucca Flat GFM followed the general workflow listed below:

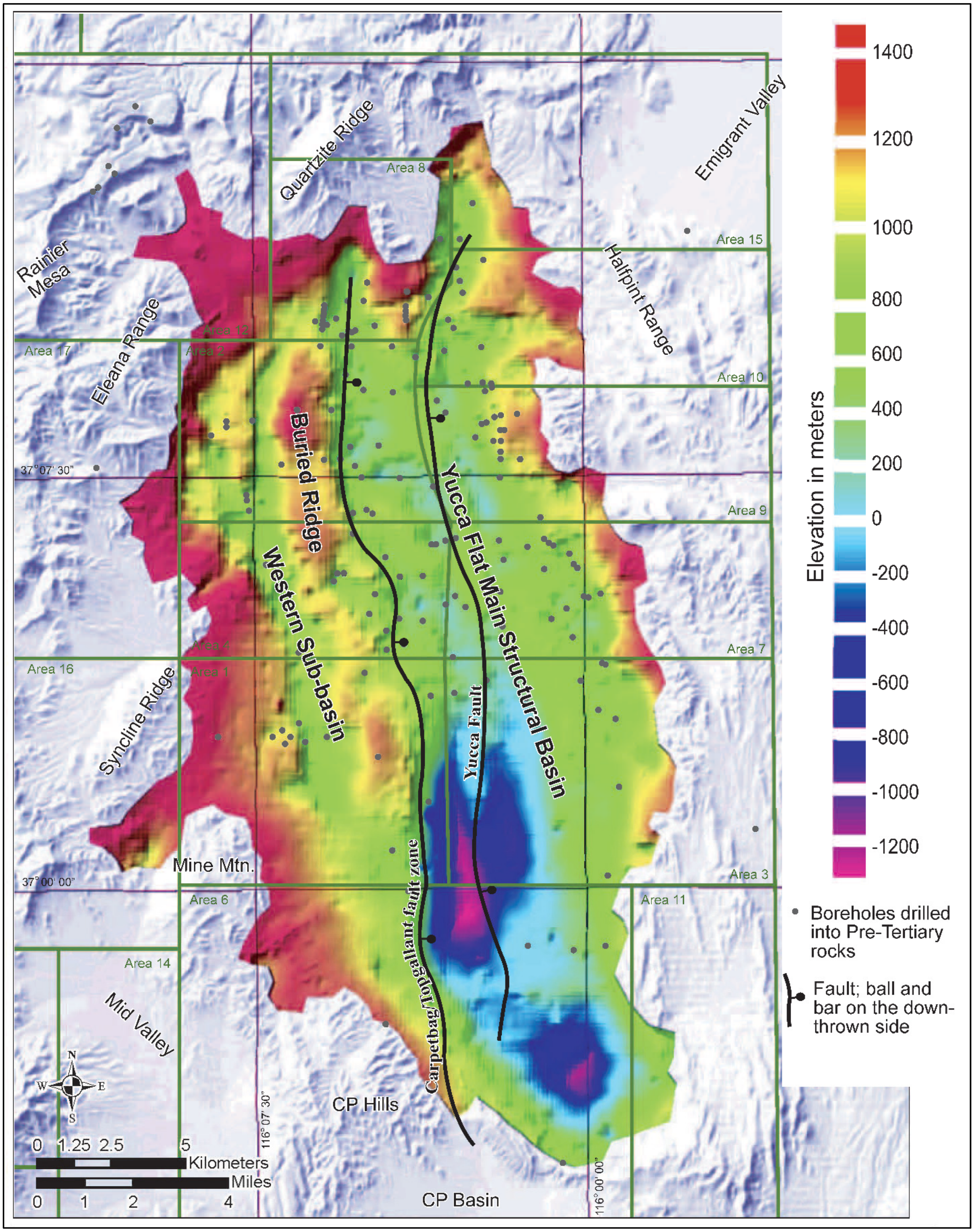

Figure 6
Color Elevation Relief Map of the Pre-Tertiary Surface beneath Yucca Flat Based on Gravity Data
(Modified from Phelps et al. 1999)

1) Determine purpose of model and establish model objectives
2) Determine model extents (i.e., lateral and vertical dimensions)
3) Develop conceptual stratigraphic system and determine model layers
4) Develop conceptual structural model; determine faults to include and their structural relationships
5) Compile and format input data files
6) Import data into EarthVision and build model
7) Perform quality control (QC) check of data import
8) Review model and revise as necessary

The DAG Yucca Flat GFM was constructed using the projection Universal Transverse Mercator (UTM), Zone 11 North, North American Datum of 1927 (NAD27) with all units in meters.

3.2 Model Extent

The DAG Yucca Flat GFM includes all of Yucca Flat and portions of the surrounding highlands (see Figure 1). It extends 22.5 km east-west and 39.0 km north-south with a total model area of 877.5 km^2. The model extends vertically from topographic surface to –4,000 m below sea level. The highest land surface elevation in the model area is 2,348 m in the northwestern portion of the model and the lowest elevation is 1,108 m along the southern edge of the model. Table 1 lists the corner coordinates of the DAG Yucca Flat GFM.

Table 1
Coordinates of the DAG Yucca Flat GFM Area

	Coordinates (UTM, NAD27, meters)	
	Easting	Northing
Southwest Corner	570000.00	4085000.00
Southeast Corner	592500.00	4085000.00
Northeast Corner	592500.00	4124000.00
Northwest Corner	570000.00	4124000.00

3.3 Data and Other Model Input used to Construct the DAG Yucca Flat GFM

Geologic and geophysical studies of Yucca Flat have been conducted for more than 55 years, resulting in large amounts of geologic and geophysical data and a good understanding of the geology of the basin and surrounding region. Data used to construct the DAG Yucca Flat GFM are discussed below. It should be noted, however, that many of the datasets discussed below are probably better characterized as interpretive information, because they represent interpretations of raw data. For example, surface geologic maps are geologic interpretations based on field observations of rock outcroppings. Similarly, drill hole data such as stratigraphy, lithology, alteration, and elevation of units penetrated by drill holes are interpreted from drill cuttings, core samples, and geophysical well logs.

3.3.1 Digital Elevation Model

Topography of the model area was represented by an EarthVision two-dimensional (2-D) gridded surface generated from a 10-m digital elevation model of the topography. During model construction the topography grid was used as an erosional layer to "carve out" the topography in the DAG Yucca Flat GFM. This helped assure that no model layers would be deposited above the topography, and also provided more precise realizations of the outcrop and extent of surface units. In addition, exporting the topography 2-D binary grid as an ASCII data file (x-y-z point data) allowed for the capture of elevation points that define the surface exposures (i.e., outcrop) of model layers. EarthVision polygon files defining the surface exposures of each model layer were created from ArcGIS shape files extracted from Slate et al. (1999). The polygon files were used to capture the surface elevation points from the ASCII topography data corresponding to the surface occurrence of each layer. These surface data points were added to the input data files for each model layer.

3.3.2 Geologic Maps

The surface geology of the NNSS and vicinity was systematically mapped by the United States Geological Survey (USGS) during the 1960s. This mapping effort resulted in a series of high quality, internally consistent geologic quadrangle maps published at a scale of 1:24,000, and established the basic stratigraphic and structural relationships of the NNSS region. Slate et al. (1999) compiled these and other USGS geologic maps of the region to produce a digital geologic compilation map for the NNSS and vicinity, and this compilation map was used to incorporate surface geologic information during GFM construction. A geo-referenced image of Slate et al. (1999) was used to determine surface exposures of model layers. The geo-referenced image was draped over the top of the EarthVision model to QC surface occurrences of model layers (Figure 7). ArcGIS polygon shapefiles of unit contacts from Slate et al. (1999) were used to capture surface (i.e., outcrop) elevation points of model layers as described in Section 3.3.1 above. The correlation of unit polygons from Slate et al. (1999) with model layers is provided in Table 2.

Table 2
Correlation of GFM Layers with Unit Polygons from Slate et al. (1999)

GFM Layer[1]	Outcrop Polygons from Slate et al. (1999)
AL	Qai, Qay, Qeo, Qp, QTa, QTc, Tgy
UWT	Tma, Tmr
VNT	Tac, Tcb, Ttb
LWT	Tpc, Tpt
ZNT	Tac[2], Tbg, Tcb[2], Tem, Tes, Tfq, Tgo, Tgp, Tn, Tob, Ton, Tor, Tot, Toy, Tpm, Trl, Tub, Tw
PZ	PPt, PMsc, Cbb, Cbp, Cc, Cn, Cz, CZw, Dg, Ds, Dsf, DSsl, MDe, MDu, Oe, Op, Zj, Zs
MZ	Kg

1. See Figure 5 for symbol definitions, and Section 4.1 for model layer descriptions.

2. In southern portion of model area only.

A map of surface effects from underground nuclear explosions in Yucca Flat (Grasso 2001) was used to evaluate and help QC the surface traces of the Yucca and Carpetbag faults.

A collection of existing subsurface geologic maps were reviewed during construction of the GFM. These maps had been constructed for select stratigraphic units in the southern portion of Yucca Flat in support of the Weapons Testing Program (WTP; Drellack 1994; 1995) and were based mainly on drill hole data. They include both isopach (i.e., thickness) and structure contour (i.e., elevation) maps, and provided important information in identifying and locating buried

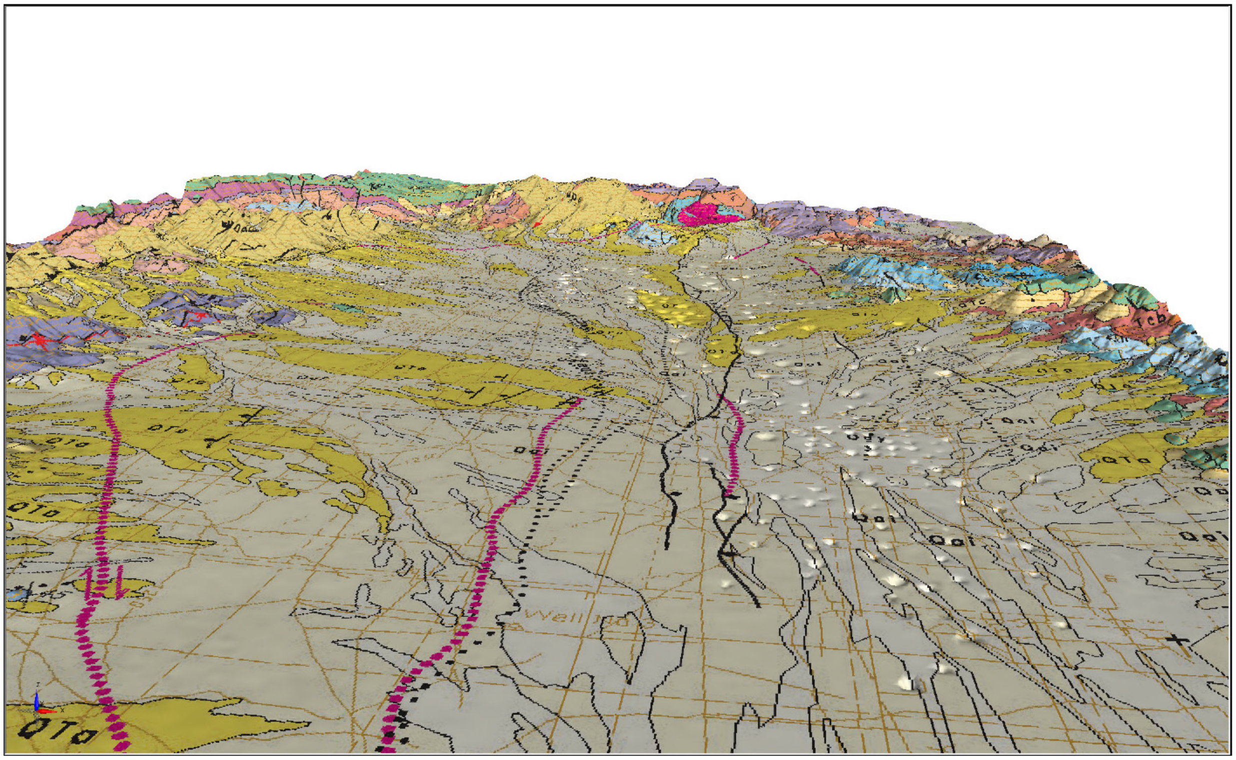

Figure 7
Perspective View Looking North at the Northern Portion of the DAG Yucca Flat GFM with the Geologic Map (Slate et. al. 1999) draped over the GFM

faults beneath southern Yucca Flat during the WTP. The structure contour map of the top of Pre-Tertiary rocks was geo-referenced and draped over the PZ model layer to evaluate and help QC fault locations on top of the PZ layer.

3.3.3 Drill Hole Data

The DAG Yucca Flat GFM incorporates information from 956 drill holes (Figure 8). These drill holes provide subsurface elevation tops for model layers, are critical input data for modeling the subsurface distribution of model layers beneath Yucca Flat, and provide controls on buried fault locations and offsets. Drill hole data, along with outcrop exposures, also provide the fundamental information for establishing model layers through the rigorous integration of stratigraphic, lithologic, fracture, and secondary alteration data (see Section 4.1 below).

Initial drill hole data were extracted from Appendix A of the UGTA hydrostratigraphic framework model documentation report for Yucca Flat (BN 2006), and revised and modified as appropriate for this modeling effort based on information from Wood (2007), Raytheon Services Nevada (1990), Drellack and Thompson (1990), and Pawloski (1997). The number of holes was also increased significantly from the UGTA modeling effort (BN 2006) to include holes that were not utilized in the UGTA model because they provide only limited data (e.g., holes that bottom in alluvium). Table 3 shows the number of drill hole penetrations for each of the model layers.

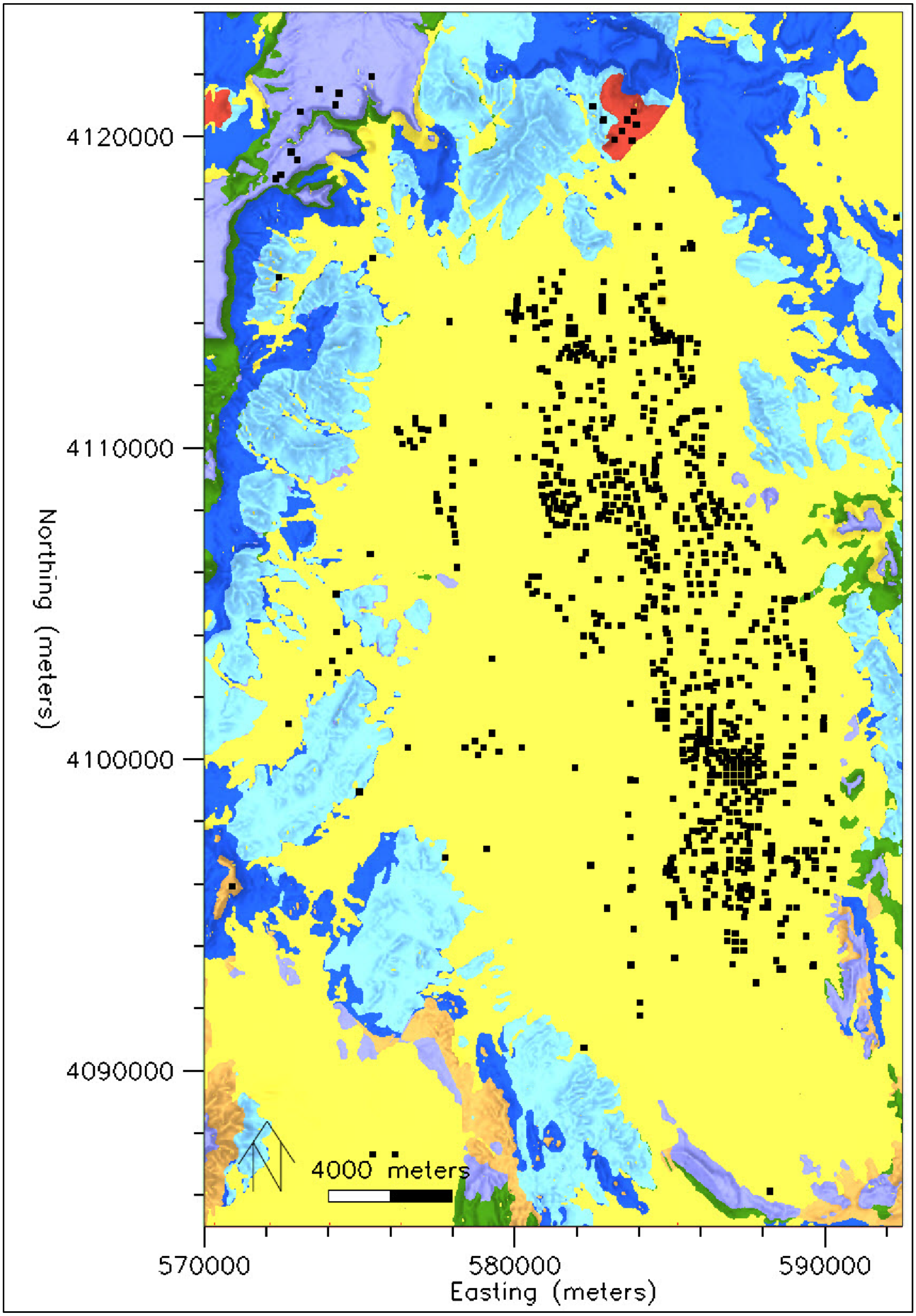

Figure 8
Map View of the DAG Yucca Flat GFM Showing Locations of Drill Holes (black squares) used in Model Construction

Table 3
Number of Drill Hole Penetrations for GFM Layers

GFM Layer	Number of Drill Hole Penetrations		
	Layer Top Penetrations	Full Penetrations	Partial Penetrations
AL	935	596	339
UWT	311	247	64
VNT	492	356	136
LWT	30	21	9
ZNT	334	138	196
PZ	203	none	203
MZ	6	none	6

3.3.4 Geophysical Data

Existing geophysical data for the model area are abundant, and include gravity, magnetic, and seismic. Much of the geophysical data provided the initial interpretations of the Yucca Flat subsurface prior to extensive drilling of the basin. Because of the current abundance of drill hole data for much of Yucca Flat, geophysical data were mainly utilized in GFM construction as input to model the top of the Paleozoic rocks in areas of sparse drill hole control. This included elevation points for the top of Paleozoic rocks as interpreted from seismic reflection surveys (Wagoner 2014) and gravity data (Cole et al. 1997 and Phelps et. al. 1999). A structure contour map, including fault locations, of the Pre-Tertiary surface beneath Yucca Flat based on gravity and drill hole data (Cole et al. 1997) was geo-referenced and draped over the PZ model layer to evaluate and help QC surface elevations and fault locations. The subsurface shape and extent of the granitic intrusion in the northern portion of the model area is based almost exclusively on geophysical data.

3.3.5 Existing Models

As mentioned previously, the DAG Yucca Flat GFM integrates concepts and components of two existing geologic framework models of the Yucca Flat region. Both GFMs were constructed in EarthVision and are briefly described below.

3.3.5.1 SPE Phase I GFM

A legacy GFM of the Yucca Flat region was constructed by Lawrence Livermore National Laboratory (LLNL) starting in the middle 1990s. This legacy model was used for SPE Phase I conducted in granite at the northern end of Yucca Flat (Wagoner 2014). This legacy GFM consists of 4 model layers and up to 220 faults. Model layers from highest to lowest are alluvium, Tertiary volcanic rocks, Pre-Tertiary sedimentary rocks, and Mesozoic granite. The DAG Yucca Flat GFM incorporates the fault structure of the northern half of Yucca Flat from this SPE Phase 1 GFM. To simplify model construction and manipulation and to be more consistent with the fault structure used for the southern half of Yucca Flat (see discussion below), a subset of the SPE Phase 1 GFM faults was applied for the DAG Yucca Flat GFM. This subset included the larger faults judged to potentially be the most significant to seismic wave propagation modeling. SPE Phase 1 GFM input data files for topography, PZ outcrop, and elevation tops defining the MZ model layer were utilized as input for the DAG Yucca Flat GFM.

3.3.5.2 UGTA Yucca Flat Hydrostratigraphic Framework

As part of the Underground Test Area project (UGTA), a 3-D GFM for the Yucca Flat region was constructed in 2006 to aid in the development of groundwater flow and contaminant transport models of underground nuclear testing areas in Yucca Flat (BN 2006). The UGTA GFM, referred to as a hydrostratigraphic framework model (HFM), is geology-based and employs stratigraphic principles and rock properties to group the various rock layers beneath Yucca Flat into model layers based on their overall ability to transmit ground water. The Yucca Flat HFM includes 25 model layers and 178 faults. Of particular interest and value to construction of the DAG Yucca Flat GFM, were the model layers established for the volcanic rock section in the UGTA HFM. A similar subdivision of the volcanic rock section was an initial desire of the DAG Yucca Flat GFM to increase resolution within the volcanics beyond that of the SPE Phase I GFM.

Because many of the properties and characteristics that control and influence a rock's ability to transmit groundwater, such as density, porosity, and propensity to fracture, are among the properties and characteristics that influence the transmission of seismic waves through the rocks, the Yucca Flat HFM has many components that are relevant and directly applicable to the DAG Yucca Flat GFM (Prothro et. al. 2015). As a result, selected data and information from the UGTA HFM were applied directly, or with only minimal modification, for the DAG Yucca Flat GFM. This mainly included modeled elevation tops of layers and elevation tops from drill holes. In addition, much of the fault structure in the UGTA HFM for the southern half of Yucca Flat was incorporated into for the DAG Yucca Flat GFM.

3.3.6 Control Points

Control points are x-y-z data points manually created to facilitate more realistic and accurate modeling, particularly in areas of sparse data control. They are typically used to help assure modeling conforms to conceptual geologic models (e.g., dip-slip offset on normal faults), and precisely to "hard" data such as surface outcrop and partially penetrating drill holes.

4.0 Model Components

A typical EarthVision geologic model consists of two main components: layers (or horizons) that represent the geologic/stratigraphic units being modeled, and faults that offset the layers and subdivide the model into fault blocks. Each of these components are defined within EarthVision as individual 2-D gridded surfaces representing the tops of model layers and the fault planes.

4.1 Model Layers

The DAG Yucca Flat GFM includes 7 model layers (see Figure 5). The process of defining model layers for the DAG Yucca Flat GFM generally followed the same process as described in Prothro et al. (2009a) for defining model layers in UGTA hydrostratigraphic framework models. The DAG Yucca Flat GFM layers consist of groupings of rocks with similar physical properties (e.g., porosity, density, strength, and propensity to fracture). These properties are mainly a function of the rock's primary lithology and the degree of secondary (post-depositional) alteration that has affected the rocks. Thus, the rocks of the model area were first grouped into what can be thought of as "physical property units" based on the lithologic characteristics that are the main determinates of a rock's physical properties. Stratigraphic information and concepts were then applied to assure these units correlated correctly across the model area. The resulting units became the layers in the model. This methodology is illustrated in Figure 9 using drill hole U-7aq. The model layers are listed with abbreviated descriptions in Table 4. Note that some model layers have the same name as physical property units because no stratigraphic descriptor (e.g., upper, lower) is necessary to differentiate some model layers from other layers with similar physical properties. More detailed descriptions of the layers are provided below in order from the highest to lowest layer in the model. For a visual reference for layer relationships see Figure 5. Quantitative data on physical properties of the layers are provided in Appendix A.

Table 4
Layers in the DAG GFM
(Listed in descending model order)

GFM Layer	Main Stratigraphic Unit(s)[1]	Basic Lithology	General Physical Properties[2]
Alluvium (AL)	Qp, QTe, Tyb, QTa	Mostly sand and gravel, lesser fine-grained playa deposits, very minor basalt.	Low density and high porosity. Poorly fractured.
Upper welded tuff (UWT)	Tma, Tmr	Devitrified welded ash-flow tuff.	Relatively high density and low porosity. Moderately to well fractured.
Vitric nonwelded tuff (VNT)	Variable[3]	Vitric nonwelded ash-flow tuff, and bedded ash- and pumice-fall deposits and reworked tuff.	Relatively low density and high porosity. Typically poorly fractured.
Lower welded tuff (LWT)	Tpc, Tpt	Devitrified moderately to densely welded ash-flow tuff.	Relatively high density and low porosity. Moderately to well fractured.
Zeolitic nonwelded tuff (ZNT)	Variable[3]	Zeolitic bedded ash- and pumice-fall deposits, lesser partially welded tuff.	Relatively moderate density and high porosity, but low permeability. Typically poorly to moderately fractured.
Paleozoic rocks (PZ)	PC, C-D, MDe	Mostly carbonate rocks; lesser siliciclastics.	Very high density and very low porosity. Well fractured.
Mesozoic granitic rocks (MZ)	Kg	Quartz monzonite and granodiorite.	Very high density and very low porosity. Well fractured.

Notes:
1. See Figure 5 for definition of stratigraphic symbols.
2. See Appendix A for quantitative physical property data.
3. Dependent on geographic location and stratigraphic level of the top of pervasive zeolitization.

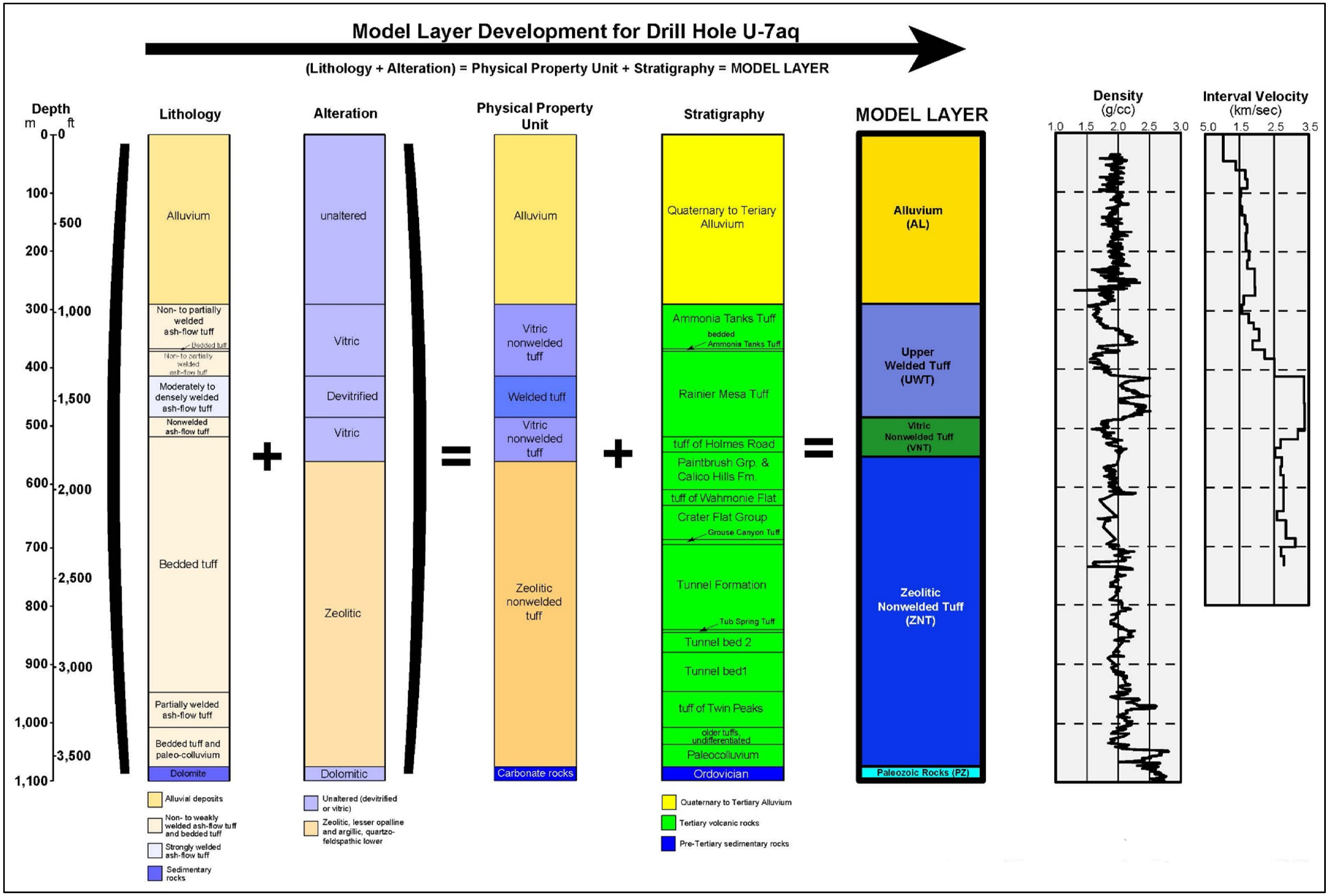

Figure 9
Methodology for Developing Model Layers

4.1.1 Alluvium (AL)

The uppermost layer in the GFM is the AL. This layer includes material eroded from adjacent highlands that was deposited as basin fill, colluvium, and modern stream/wash deposits, generally during the last 10 million years and in response to the development of the Yucca Flat basin. The AL typically consists of friable to moderately consolidated, poorly sorted mixtures of volcanic and sedimentary rock debris ranging in particle size from clay to boulders. Minor amounts of eolian (i.e., windblown) sand and basalt flows are also present in the AL. Thick intervals of clayey to silty playa deposits occur within the AL at the southern end of Yucca Flat.

4.1.2 Upper Welded Tuff (UWT)

The UWT consists mostly of welded ash-flow tuff and lesser nonwelded and bedded tuff. Ash-flow tuffs are volcanic rocks explosively erupted and deposited by highly fluid density currents consisting of hot gas and glassy (i.e., vitric) ash with lesser amounts of small felsic and mafic crystals and rock fragments (Fisher and Schmincke 1984; Cas and Wright 1987). Ash-flow tuffs, like those of the UWT, can be regional in extent, and blanket large areas with thick deposits. An aspect of ash-flow tuffs important to their physical properties is the degree of welding that occurs shortly after deposition. In many instances as ash-flow tuffs cool, they compact, or weld, which can result in a significant increase in density and reduction in matrix porosity. This can also result in a much harder and stronger rock than that originally deposited. The welding process also typically results in devitrification (i.e., crystallization) of the original vitric components to microcrystalline quartz and feldspar. In most welded ash-flow tuffs, the degree of welding tends to increase towards the center of the deposit, and thus, physical properties will not be distributed isotropically in welded ash-flow tuffs but vary relative to the degree of welding.

Ash-flow tuffs also volumetrically contract as they cool, which typically produces fractures called cooling joints (Fisher and Schmincke 1984; Cas and Wright 1987). These joints can form interconnected, systematic fracture sets that cluster in different portions of the deposit. Tectonic fractures are also common in welded ash-flow tuffs due to their more consolidated and brittle character. Thus, welded ash-flow tuff tends to be moderately to well fractured.

The UWT in the DAG Yucca Flat GFM consists predominantly of the welded portion of the Rainier Mesa Tuff. The basal nonwelded ash-flow portion of the Rainier Mesa Tuff is included within the underlying vitric nonwelded tuff (VNT) model layer described in the following section. The UWT also includes rocks of the overlying Ammonia Tanks Tuff where present. These rocks include welded and nonwelded ash-flow tuff and bedded tuff, and typically account for only a minor portion of the UWT.

The UWT is present in most of the central and southern portions of the main Yucca Flat basin east of the buried Paleozoic ridge. The unit is not present in the northern portion of Yucca Flat or on the higher portions of the buried Paleozoic ridge. It has limited occurrence in the western sub-basin west of the buried ridge. The UWT caps much of the higher terrain northwest and southeast of Yucca Flat. The UWT was encountered in 311 drill holes in Yucca Flat, of which 247 fully penetrated the unit. In these full penetrations, the UWT ranges in thickness from 15 m to just over 300 m, with an average thickness of 108 m.

4.1.3 Vitric Nonwelded Tuff (VNT)

The VNT consists primarily of massive to thinly bedded ash- and pumice-fall deposits, reworked tuff, and nonwelded ash-flow tuff. Most of these deposits are ash cloud fall-out deposits and are typically dominated compositionally by vitric (i.e., unaltered) ash and pumice, and lesser amounts of small quartz and feldspar crystals, mafic minerals such as biotite and hornblende, and rock fragments.

Because the rocks composing the VNT were originally deposited as relatively thin beds and under relatively cool conditions, they did not undergo welding and the associated compaction and porosity reduction, as observed in ash-flow tuffs. Thus, they are relatively low-density and high-porosity rocks. In addition, the VNT tends to be poorly fractured due to the general absence of cooling joints and its low strength, which tends to accommodate deformation through grain crushing, grain boundary sliding, and associated porosity reduction (Prothro et al. 2009b; Wilson et al. 2003). The poorly fractured nature of the VNT results in the majority of the VNT being a single porosity unit dominated by primary matrix porosity.

Typically, the VNT includes all volcanic units from the base of welded Rainier Mesa Tuff (UWT) to the top of pervasive zeolitization (secondary alteration). Where the UWT is not present, the top of VNT corresponds to the base of the overlying AL. In some areas where zeolitization has not occurred, the VNT extends down to the top of PZ. In the southern portion of Yucca Flat, VNT directly overlies welded Topopah Spring Tuff (LWT). Here the basal portion of the VNT tends to be zeolitic. The thickness of zeolitic rocks at the base of the VNT where it overlies LWT is typically less than 20 m, based on drill hole penetrations.

The VNT is a widespread unit throughout the model area and underlies most of Yucca Flat. Like other volcanic units, it is not present on the higher portions of the buried Paleozoic ridge that runs beneath the western portion of the basin. In Yucca Flat, the VNT is encountered in 492 drill holes, 356 of which fully penetrate the unit. In these full penetrations, the VNT ranges in thickness from less than a meter to over 450 m in U-10c #1, with an average thickness is 354 m.

4.1.4 Lower Welded Tuff (LWT)

The LWT is present only in the southern portion of the model area. In southern Yucca Flat it consists of welded ash-flow tuff of the Topopah Spring Tuff. In the southwest portion of the model area, however, the LWT also includes younger but closely related welded Tiva Canyon Tuff and minor bedded tuff that occurs between the two formations. Like the UWT, the LWT is a relatively high-density, low-porosity unit that is moderately to well fractured.

The LWT is encountered in 30 drill holes with 21 penetrating completed through the unit. Beneath southern Yucca Flat, the LWT is relatively thin, averaging 60 m thick in drill holes that penetrate a complete thickness of the unit. Two drill holes in Mid Valley located in the southwestern portion of the model area encountered the LWT. The LWT outcrops in many of the highland areas in the southern portion of the model area.

4.1.5 Zeolitic Nonwelded Tuff (ZNT)

The ZNT consists primarily of massive to thinly bedded ash- and pumice-fall deposits, reworked tuff, and nonwelded ash-flow tuff and, thus, is similar to the VNT in basic volcanic lithology. However, the original vitric components (e.g., ash and pumice) of most of the rocks of the ZNT have undergone low-temperature secondary alteration in the form of zeolitization. This alteration process occurred well after the tuffs were deposited and in the presence of ground water (Hoover 1968). The zeolite mineral clinoptilolite is the dominant secondary alteration product in the upper portions of the ZNT. At deeper levels, the zeolite minerals mordenite and analcime become more common as clinoptilolite content decreases (Prothro 2005). At the deepest levels of the ZNT, zeolitic alteration becomes subordinate to quartzo-feldspathic and argillic alteration. The lower portion of the ZNT is also somewhat more variable lithologically, with intercalated discontinuous ash-flow tuffs, some of which are at least partially welded. Argillic paleocolluvium of variable thickness is common at the base of the ZNT.

Although similar in basic rock type, the presence of pervasive alteration within rocks of the ZNT results in some differences in physical properties compared to those for the unaltered VNT. These include generally higher density, strength, and velocity values for the ZNT compared to the VNT. Although there is a slight corresponding decrease in porosity for ZNT, permeability relative to groundwater flow is greatly reduced in the ZNT relative to the VNT (Winograd and Thordarson 1975).

In the southern portion of Yucca Flat where LWT is present, the ZNT includes all volcanic rocks from the base of the LWT to the top of PZ. Where LWT is not present, ZNT includes all rocks from the top of pervasive zeolitization to the top of PZ. The top of ZNT within the model area was encountered in 334 drill holes, with 138 penetrating completely through the unit. The maximum thickness of ZNT encountered in a drill hole is 634 m in a partially penetrating drill hole. In holes that fully penetrate the ZNT, the unit ranges in thickness from a meter to 596 m, with an average thickness of 246 m.

4.1.6 Paleozoic Rocks (PZ)

The PZ model layer consists of sedimentary and metasedimentary rocks ranging in age from approximately 270 million to 1 billion years old, and thus includes units of Paleozoic and late Precambrian age. In general, the upper portion of the PZ is dominated by carbonate rocks (limestone and dolomite) and lesser siliciclastic rocks (sandstone, siltstone, quartzite, and conglomerate) and the lower portion by siliciclastic rocks. However, this simplified stratigraphic section has been considerably shuffled by compressional deformation (folding and thrust faulting) more than 100 Ma, particularly in the western half of the model area, including beneath the western portion of Yucca Flat. The stratigraphic variability and geologic complexities described above in very general terms is not captured in the GFM. Except where intruded by Mesozoic granitic rocks in the northern portion of the model area, the PZ layer underlies the entire model area and functions as the basal layer in the GFM.

The PZ is extensively exposed in the highlands bordering Yucca Flat. The top of the layer has been penetrated by 203 drill holes in the model area.

4.1.7 Mesozoic Granitic Rocks (MZ)

Mesozoic granitic rocks consisting of quartz monzonite and granodiorite intrude older Paleozoic and Precambrian rocks in the far northern portion of the model area. These igneous intrusive rocks are approximately 100 million years old (Slate et al. 1999) and include two separate but genetically related deep-seated and steep-sided stocks. These are modeled together as the

Mesozoic granitic rocks (MZ) layer. Although younger than the PZ model layer, the MZ layer is modeled as the lowermost layer in the GFM due to its intrusive nature.

4.2 Faults

The DAG Yucca Flat GFM includes 48 faults (Figure 10). Almost all the faults are buried (no surface scarp) and all are likely related to basin development. These and other buried faults were identified during the decades of geological and geophysical work in Yucca Flat for the WTP. Data and information used to identify buried faults included surface fracturing caused by underground nuclear explosions, geophysical data such as gravity and seismic reflection, and subsurface mapping of units penetrated by drill holes.

To simplify model construction, a subset of the known faults was used. These faults include the main basin-forming faults, such as the Yucca, Carpetbag, and Topgallant faults, as well as other faults that together control and define the main structural grain and basin architecture. Faults are typically modeled with 75 degree dip and normal (dip-slip) displacement. Since the major basin-forming faults in Yucca Flat are east-dipping, west-dipping faults are typically modeled as terminating against east-dipping faults. Faults not terminating against other faults extend to the base of the model. Because most of the faults are buried by alluvium and do not show surface scarps, all faults are modeled as terminating within the alluvium.

5.0 Model Exports

The main export format for the DAG Yucca Flat GFM is simple ASCII text that defines the model layers and faults as 2-D surfaces representing the tops of each layer and fault surface. These export files consist of a series of points correctly positioned in 3-D space (x [easting], y [northing], and z [elevation]) defining the surface. Model layers can also be exported as 3-D volumes using EarthVision's 3-D gridding algorithms. Assigning each model layer a separate property value and creating a 3-D property model results in each model layer defined as a separate 3-D volume consisting of points defined by x, y, z, and p (property). This 3-D property model is also available as a simple ASCII text file. Other export formats include binary-STL and Gocad.gp.

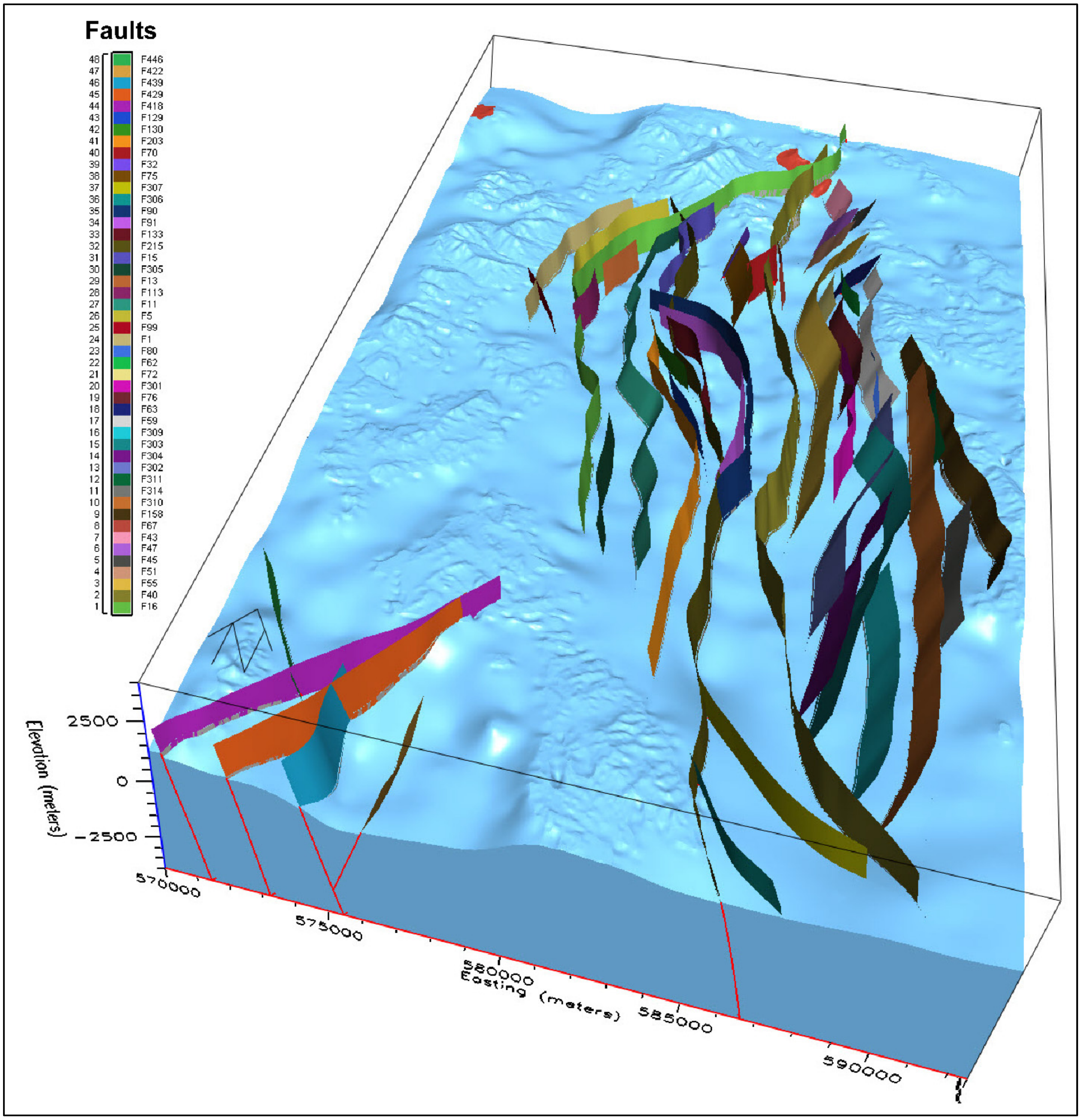

Figure 10
3-D Perspective View of the DAG Yucca Flat GFM with the Volcanic Layers and Alluvium Removed, and Showing the Faults Included in the GFM

6.0 References

Bechtel Nevada, 2006. *A Hydrostratigraphic Model and Alternatives for the Groundwater Flow and Contaminant Transport Model of Corrective Action Unit 97: Yucca Flat-Climax Mine, Lincoln and Nye Counties, Nevada.* DOE/NV/11718--1119. Las Vegas, NV.

BN, see Bechtel Nevada.

Cas, R. A. F., and J. V. Wright, 1987. *Volcanic Successions*. Allen and Unwin, London, 528 pp.

Cole, J. C., A. G. Harris, and R. R. Wahl, 1997. *Subcrop Geologic Map of Pre-Tertiary Rocks in the Yucca Flat and Northern Frenchman Flat Areas, Nevada Test Site, Southern Nevada.* U.S. Geological Survey Open-File Report 97-678, scale 1:48,000, 24 pp. Denver, CO.

Cole, J. C., and P. H. Cashman, 1999. *Structural Relationships of Pre-Tertiary Rocks in the Nevada Test Site Region, Southern Nevada.* U.S. Geological Survey Professional Paper 1607.

Drellack, S. L., Jr., 1994. "Subsurface Geologic Maps of Southern Yucca Flat." Memorandum TSP:DGP:024:95 to Distribution. Raytheon Services Nevada, Las Vegas, NV.

Drellack, S. L., Jr., 1995. "Structure Contour Map of the Pre-Tertiary Surface in Southern Yucca Flat." Memorandum TSP:DGP:116:95 to Distribution. Raytheon Services Nevada, Las Vegas, NV.

Drellack, S. L., Jr., and P. H. Thompson, 1990. *Selected Stratigraphic Data for Drill Holes in LANL Use Areas of Yucca Flat, NTS*. DOE/NV/10322--39. Fenix & Scisson, Inc., Las Vegas, NV.

Fisher, R. V. and H.-U. Schmincke, 1984. *Pyroclastic Rocks*. Springer-Verlag, Berlin, 472 pp.

Garcia, M. N., and Sharps, J. A., 1985. "Morphology of the Carpetbag fault system, Yucca Flat, Nevada," in Olsen, C. W., and Donohue, M. L., eds., Third Symposium on Containment of Underground Nuclear Explosions, Proceedings: Lawrence Livermore National Laboratory Report Conf-850953, v. 2, p. 64-71.

Grasso, D. N., 2001. *GIS Surface Effects Archive of Underground Nuclear Detonations Conducted at Yucca Flat and Pahute Mesa, Nevada Test Site, Nevada.* U.S. Geological Survey Open-File Report OFR-2001-272.

Hoover, D. L., 1968. "Genesis of Zeolites, Nevada Test Site." In: Eckel, E. B., editor. *Nevada Test Site*. Geological Society of America Memoir 110. Boulder, CO.

Jenkins, E. C., 1973. *Surface Fracturing of the Carpetbag Event, Yucca Flat, Nevada Test Site, Nevada*. U. S. Geological Survey Report USGS-474-160, 15 p. [NTS-233]

Pawloski, G. A., 1997. Unpublished stratigraphic information for drill holes in LLNL use areas in Yucca Flat.

Phelps, G. A., V. E. Langenheim, R. C. Jachens, 1999. *Thickness of Cenozoic Deposits of Yucca Flat Inferred from Gravity Data, Nevada Test Site, Nevada.* U.S. Geological Survey Open-File Report OFR-99-310.

Phelps, G. A., R. C. Jachens, B. C. Moring, C. W. Roberts, 2004. *Modeling of the Climax Stock and Related Plutons Based on the Inversion of Magnetic Data, Southwest Nevada*. U.S. Geological Survey Open-File Report OFR-2004-1345.

Prothro, L. B., 2005. *Mineralogic Zonation Within the Tuff Confining Unit, Yucca Flat, Nevada Test Site*. DOE/NV/11718--995. Bechtel Nevada, Las Vegas, NV.

Prothro, L. B., S. L. Drellack, Jr., and J. M. Mercadante, 2009a. *A Hydrostratigraphic System for Modeling Groundwater Flow and Radionuclide Migration at the Corrective Action Unit Scale, Nevada Test Site and Surrounding Areas, Clark, Lincoln, and Nye Counties, Nevada.* DOE/NV/25946--630, Las Vegas, NV.

Prothro, L. B., S. L. Drellack, Jr., D. N. Haugstad, H. E. Huckins-Gang, and M. J. Townsend, 2009b. *Observations on Faults and Associated Permeability Structures in Hydrogeologic Units at the Nevada Test Site*. DOE/NV/25946--690, Las Vegas, NV.

Prothro, L., M. Townsend, H. Huckins-Gang, S. Drellack, D. Reed, T. Kincaid, K. Day, 2015. “Three-dimensional seismic attribute model for Yucca Flat,” in *Site-Directed Research and Development*, FY 2014, National Security Technologies, LLC, Las Vegas, Nevada, 2015, 225–231.

Raytheon Services Nevada. 1990. “Nevada Test Site Drilling and Mining Summary.” Available from Mission Support and Test Services, Mercury, NV.

Sawyer, D. A., R. J. Fleck, M. A. Lanphere, R. G. Warren, D. E. Broxton, and M. R. Hudson, 1994. “Episodic Caldera Volcanism in the Miocene Southwest Nevada Volcanic Field: Revised Stratigraphic Framework, 40Ar/ 39Ar Geochronology and Implications for Magmatism and Extension.” *Geological Society of America Bulletin*, v. 106, pp. 1,304-1,318.

Slate, J. L., M. E. Berry, P. D. Rowley, C. J. Fridrich, K. S. Morgan, J. B. Workman, O. D. Young, G. L. Dixon, V. S. Williams, E. H. McKee, D. A. Ponce, T. G. Hildenbrand, WC Swadley, S. C. Lundstrom, E. B. Ekren, R. G. Warren, J. C. Cole, R. J. Fleck, M. A. Lanphere, D. A. Sawyer, S. A. Minor, D. J. Grunwald, R. J. Laczniak, C. M. Menges, J. C. Yount and A. S. Jayko, 1999. Digital Geologic Map of the Map of the Nevada Test Site and Vicinity, Nye, Lincoln, and Clark Counties, Nevada and Inyo County, California. U.S. Geological Survey Open-File Report 99B554BA, scale 1:120,000.

U.S. Geological Survey (and Nevada Bureau of Mines and Geology), 2006. Quaternary fault and fold database for the United States, accessed April 23, 2019, from USGS web site: http//earthquake.usgs.gov/hazards/qfaults/.

Wagoner, J. L., 2014. “Working toward a site-specific geomodel---Nevada National Security Site”, RMR2014–Review of Monitoring Research for Ground-Based Nuclear Explosion Monitoring Technologies, Albuquerque, New Mexico, June 18, 2014.

Wilson, J. E., L. B. Goodwin, and C. J. Lewis, 2003. “Deformation Bands in Nonwelded Ignimbrites: Petrophysical Controls on Fault-Zone Deformation and Evidence of Preferential Fluid Flow.” *Geology*, vol. 31, no. 10, pp. 837–840.

Winograd, I. J., and W. Thordarson, 1975. *Hydrogeologic and Hydrochemical Framework, South-Central Great Basin, Nevada-California, with Special Reference to the Nevada Test Site*. U.S. Geological Survey Professional Paper 712-C, 126 p. Washington, DC.

Wood, D.B., 2007. Digitally available interval-specific rock-sample data compiled from historical records, Nevada National Security Site and vicinity, Nye County, Nevada (ver. 2.2, February 2017): U.S. Geological Survey Data Series 297, 23 p., https://doi.org/10.3133/ds297.

APPENDIX A

Model Layer Factsheets for the DAG Yucca Flat Geologic Framework Model

The contents of Appendix A provide additional information and data on the model layers compiled into individual factsheets for each layer. Information and data include geologic and seismic characteristics, physical properties, statistical analyses, and photographs of outcrop exposures. Physical property data and associated statistical analyses include p-wave velocity, bulk density, and porosity. P-wave velocity values are interval velocity values calculated from down-hole geophone surveys and typically represent 15.2-m intervals. These values were extracted from tables included in paper copies of the original logs. See Prothro et al. (2015) for more discussion of these data. Density values are laboratory-derived natural-state bulk density measured mostly from core samples. These data are from Wood (2007). Porosity values are calculated and also from Wood (2007).

List of Fact Sheets

Alluvium (AL)

Stratigraphy

Quaternary–Tertiary alluvium and playa deposits.

Lithology

Mostly sandy gravel and gravelly sand. Includes playa deposits at south end of valley.

Structure

Poorly fractured. Although most faults offset the base of the unit, a few (notably the Yucca and Carpetbag faults) offset the top of the unit at the land surface.

Seismic Characteristics

In DAG area consists of a 3-layer velocity model:

0 – 30 m: 900 m/sec

30 - ~300 m: 1600 m/sec, increasing with depth

300 m – base: 2100 m/sec, more variable

Physical Properties (± 1 SD)

Down-hole geophone survey P-wave velocity:

1601 ± 497 m/s (n = 2672)

Natural-state bulk density:

1.91 ± 0.18 g/cm^3 (n = 5212)

Calculated porosity:

34.5 ± 6.6 % (n = 5212)

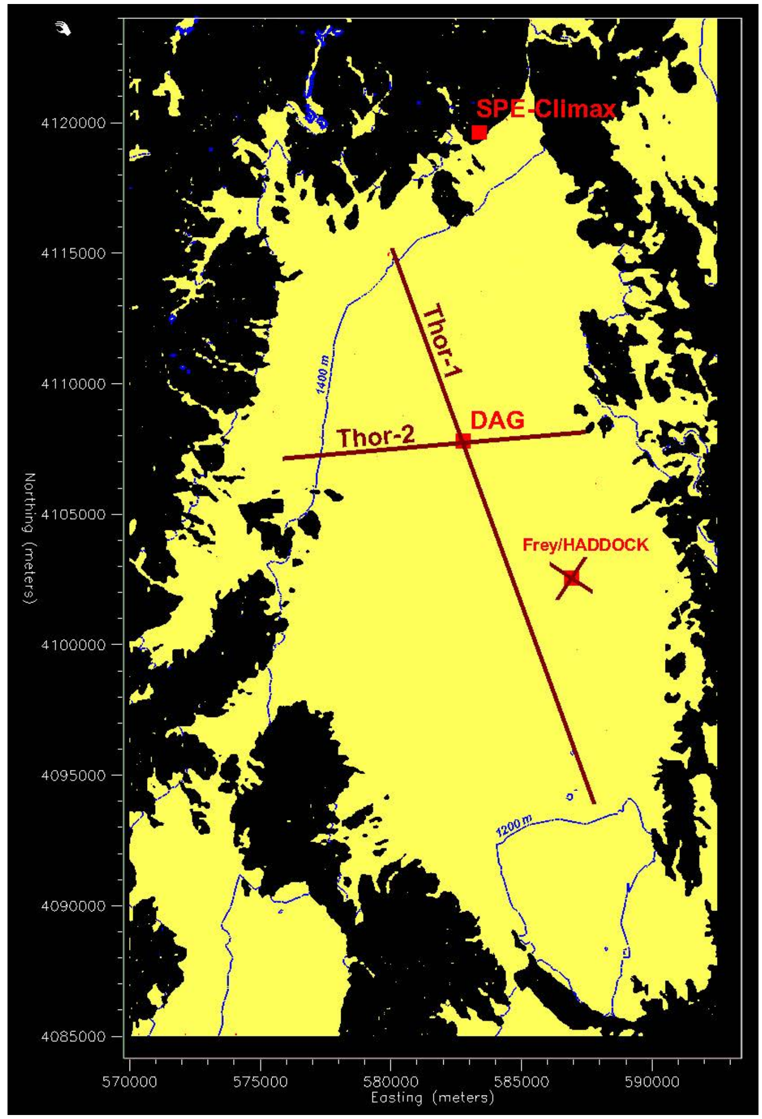

Map view of model area showing extent of AL.
Blue lines are elevation contours (interval = 200 meters)

Alluvium (AL)

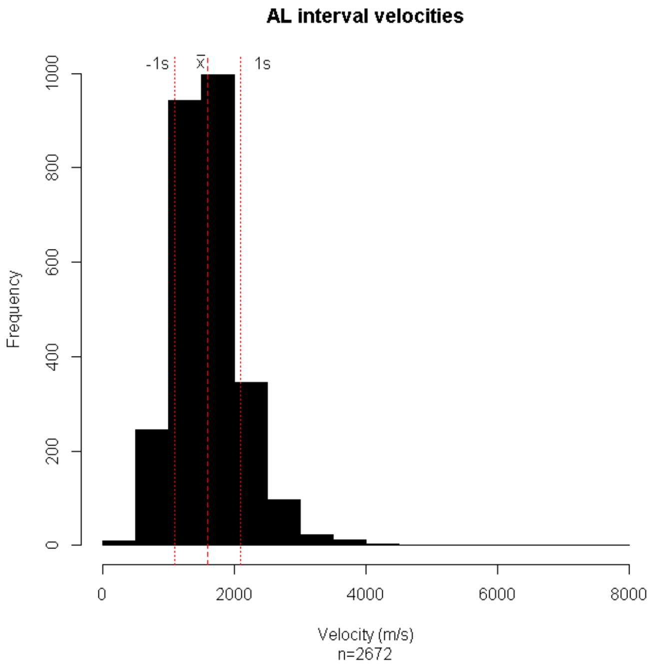
AL interval velocities
-1s
x̄
1s
Frequency
0
200
400
600
800
1000
0
2000
4000
6000
8000
Velocity (m/s)
n=2672

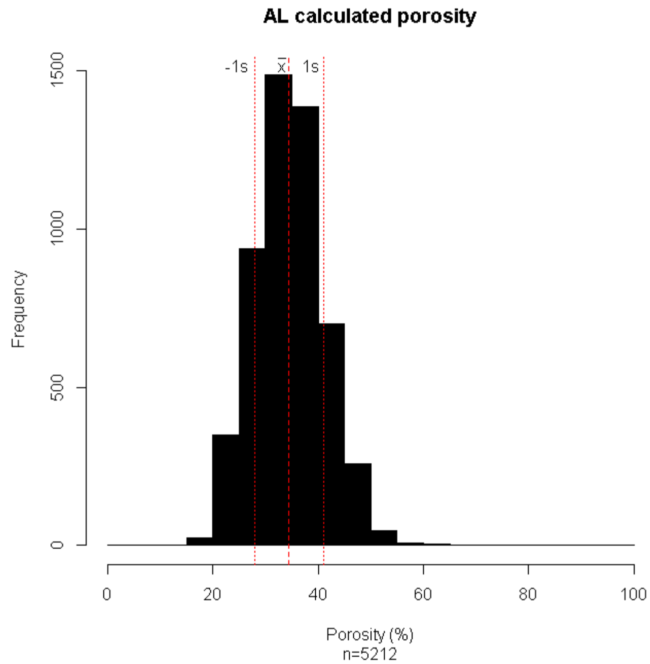
AL calculated porosity
-1s
x̄
1s
Frequency
0
500
1000
1500
0
20
40
60
80
100
Porosity (%)
n=5212

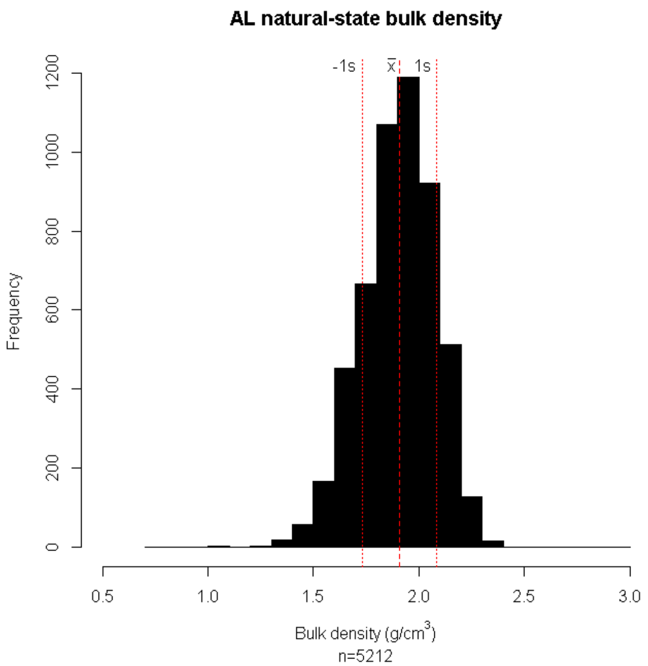
AL natural-state bulk density
-1s
x̄
1s
Frequency
0
200
400
600
800
1000
1200
0.5
1.0
1.5
2.0
2.5
3.0
Bulk density (g/cm3)
n=5212

Alluvium (AL)

Photographs

Outcrop of alluvium along wash in Area 5, NNSS.

Close-up of gravelly alluvium, Area 5, NNSS.

Alluvium exposed in the U1a Complex (~274 m below ground surface), Area 6, NNSS.

Upper Welded Tuff (UWT)

Stratigraphy

Rainier Mesa Tuff and Ammonia Tanks Tuff

Lithology

Devitrified welded tuff, includes vitric nonwelded tuff mainly in upper part.

Structure

Welded tuff portion moderately to well fractured, likely highly fractured near faults. Vitric, nonwelded tuff portions are poorly fractured.

Seismic Characteristics

Surprisingly, a relatively low-velocity unit considering welded ash-flow tuff comprises much of the unit. In many places includes a significant portion of nonwelded tuff in upper portion which may account for the overall lower velocity. Velocity will vary vertically due to varying degrees of welding, and thus internal velocity inversions are likely present. Unit as a whole may represent a velocity inversion due to lower velocity units above and below (AL and VNT respectively). Moderately to well fractured which may also partly explain lower velocity.

Physical Properties (± 1 SD)

P-wave velocity:

1982 ± 567 m/s (n = 535)

Natural-state bulk density:

1.73 ± 0.20 g/cm^3 (n = 1077)

Calculated porosity:

40.2 ± 8.6 % (n = 1083)

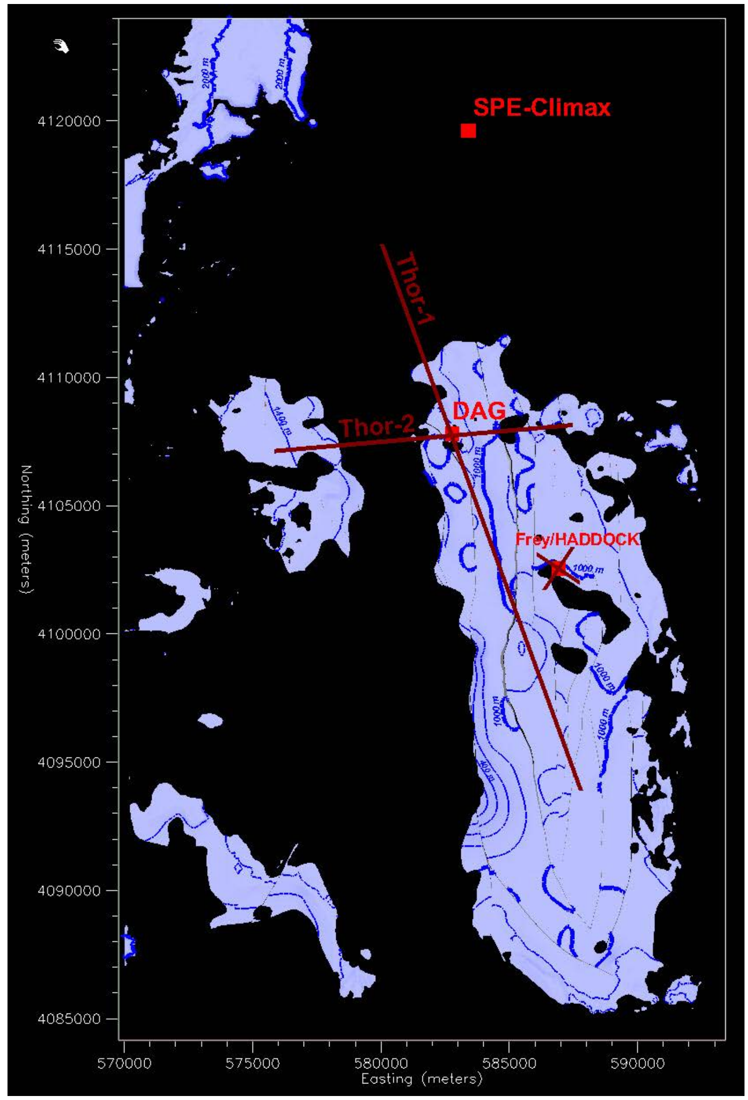

Map view of model area showing extent of UWT.
Blue lines are elevation contours (interval = 200 meters)

Upper Welded Tuff (UWT)

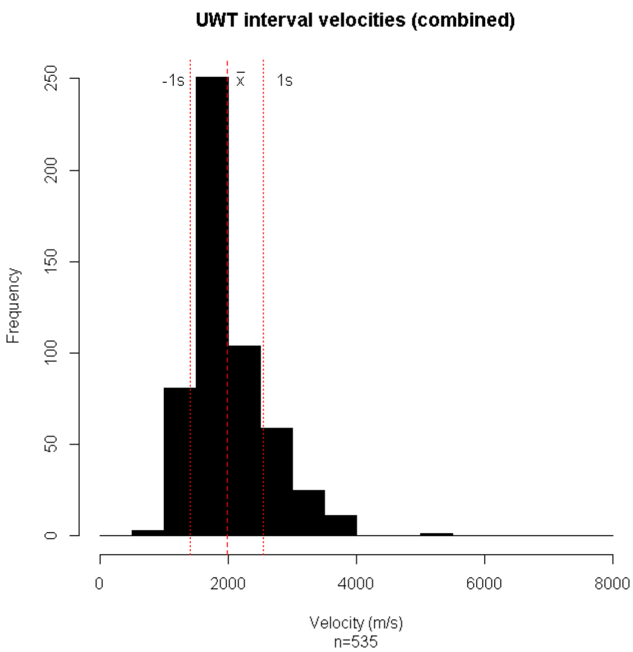

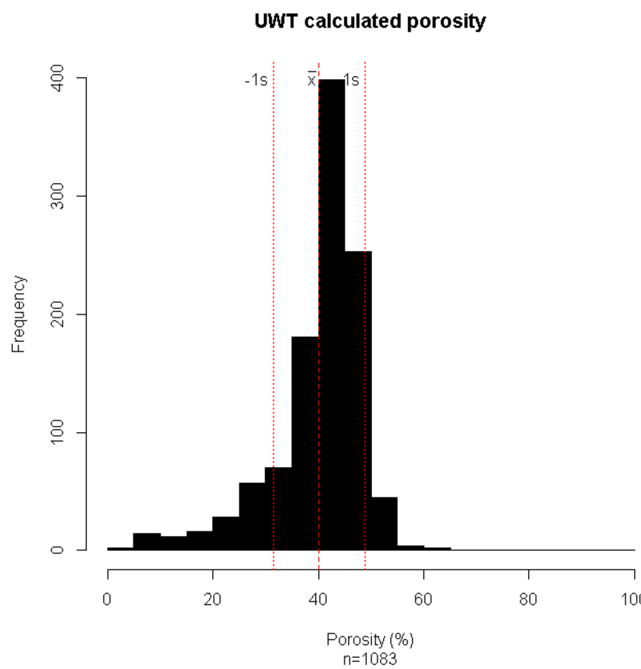

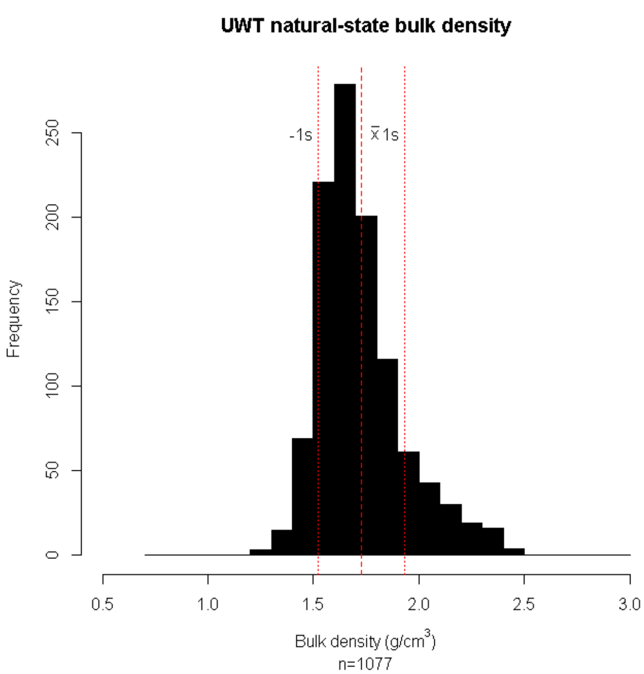

Upper Welded Tuff (UWT)

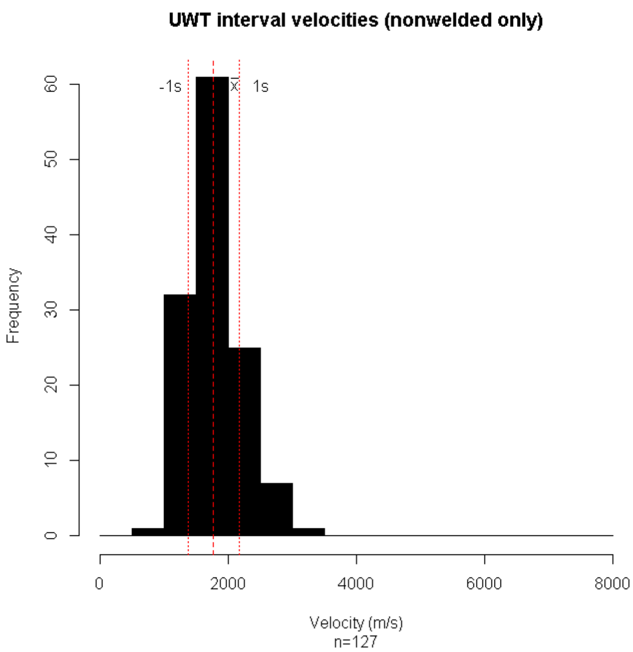

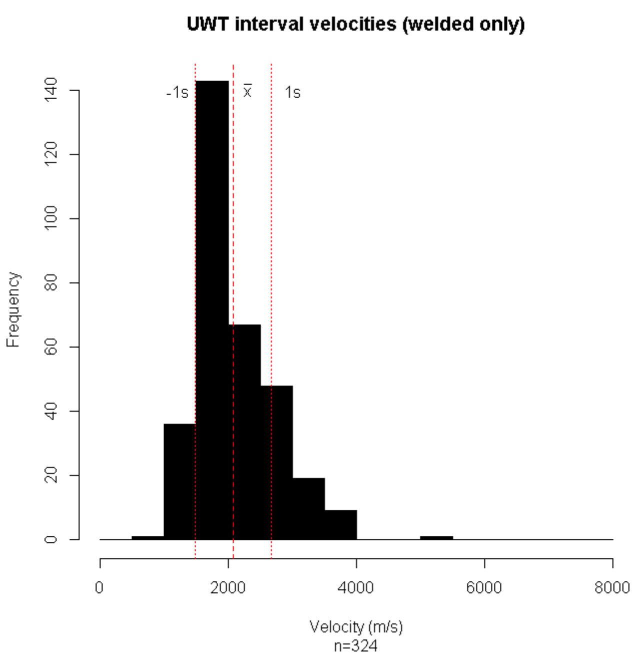

Upper Welded Tuff (UWT)

Photographs

UWT outcrop (above red line), Area 12, NNSS.

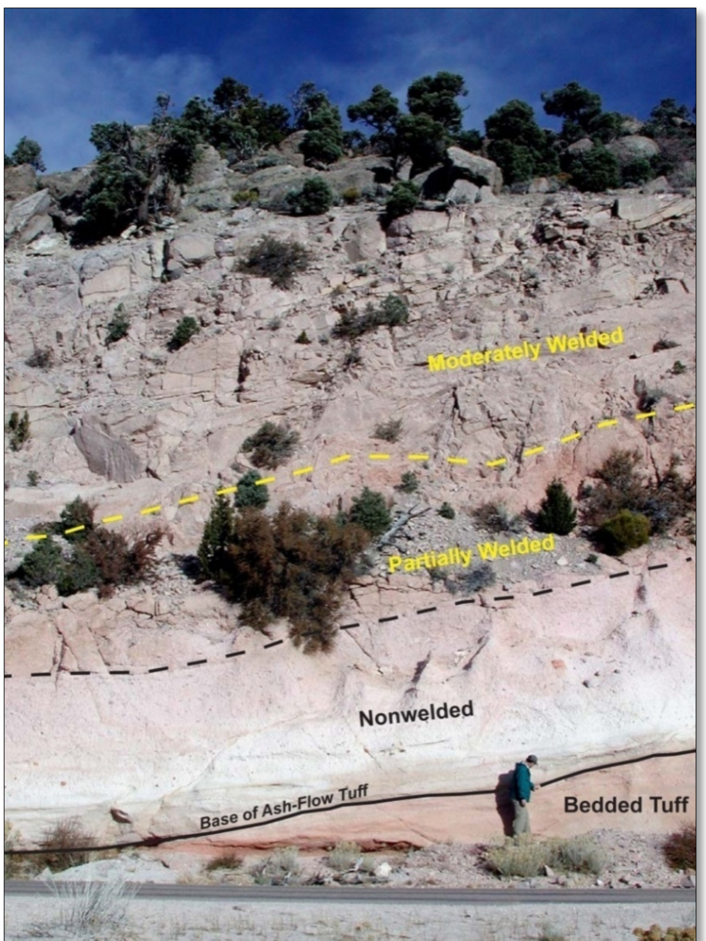

Rainier Mesa Tuff in roadcut showing welding zones within ash-flow tuff, Area 19, NNSS. UWT is above black dashed line.

Vitric Nonwelded Tuff (VNT)

Stratigraphy

In southern portion of model area, VNT includes all stratigraphic units from the base of welded Rainier Mesa Tuff (UWT) to the top of welded Topopah Spring Tuff (LWT). In northern portion of model area where LWT is not present, VNT includes all stratigraphic units from the base of welded Rainier Mesa Tuff (UWT) to the top of pervasive zeolitization (ZNT).

Lithology

Vitric (i.e., unaltered) nonwelded tuffs

Structure

Poorly fractured

Seismic Characteristics

Relatively low-velocity and somewhat isotropic unit. No significant velocity inversions present. Forms a zone of low reflectivity and low energy.

Physical Properties (± 1 SD)

P-wave velocity:

1937 ± 529 m/s (n = 756)

Natural-state bulk density:

1.65 ± 0.17 g/cm^3 (n = 2098)

Calculated porosity:

43.5 ± 6.8 % (n = 2099)

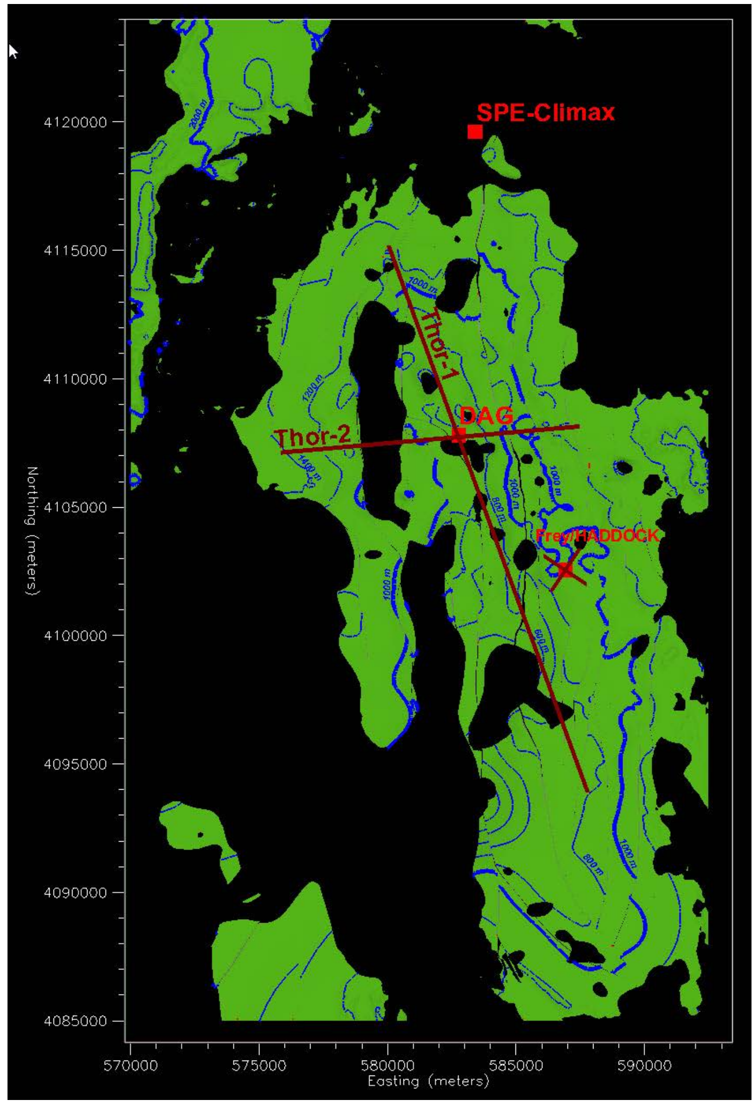

Map view of model area showing extent of VNT.
Blue lines are elevation contours (interval = 200 meters)

Vitric Nonwelded Tuff (VNT)

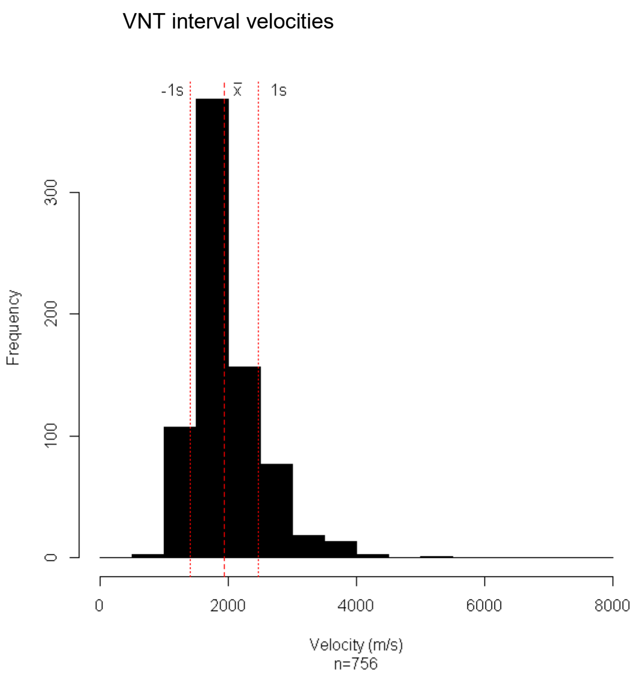

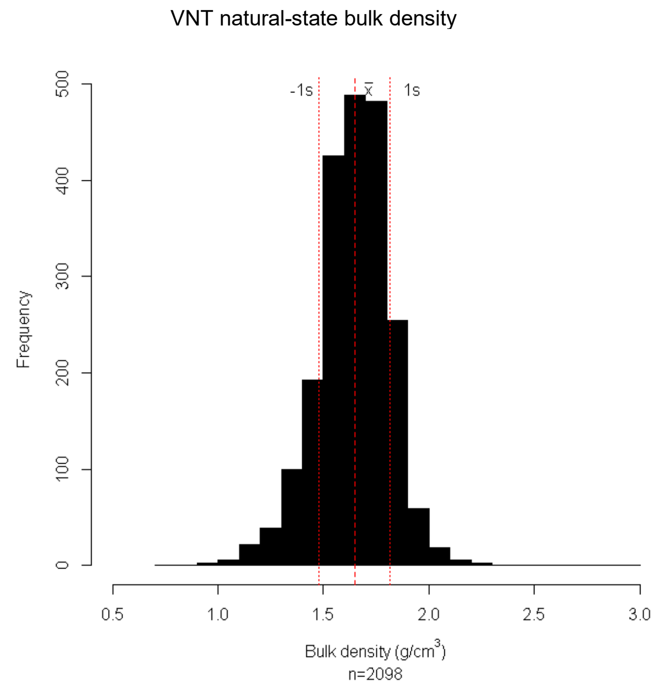

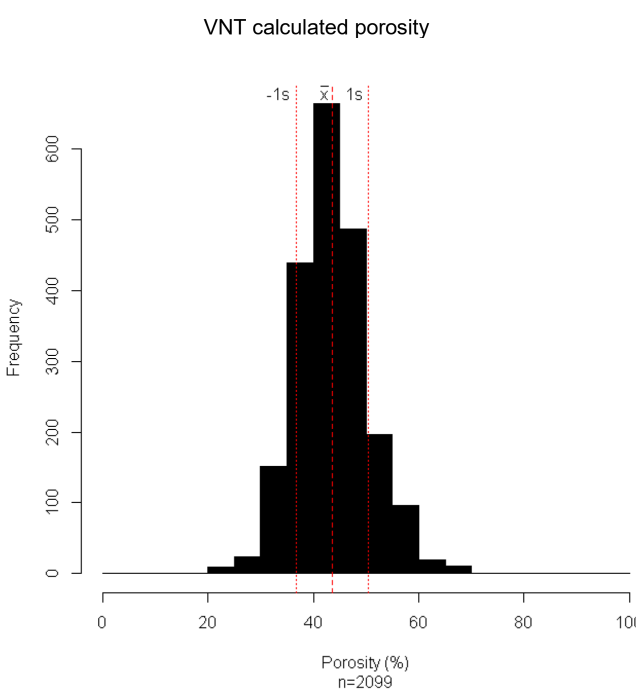

Vitric Nonwelded Tuff (VNT)

Photographs

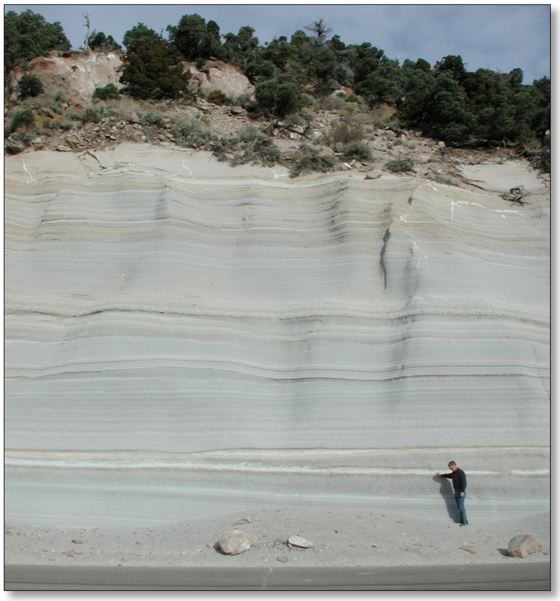

Road cut in bedded vitric nonwelded tuff, Area19, NNSS.

Outcrop of vitric nonwelded tuff, Area 20, NNSS.

Close-up of vitric nonwelded tuff.

Lower Welded Tuff (LWT)

Stratigraphy

Topopah Spring Tuff; includes Tiva Canyon Tuff in southwest portion of model area.

Lithology

Partially to densely welded ash-flow tuff.

Structure

Moderately to well fractured.

Seismic Characteristics

Relatively high-velocity zone that may represent a velocity inversion due to lower velocity units above and below (VNT and ZNT respectively). Velocity likely to vary vertically due to varying degrees of welding within unit, and thus likely contains internal velocity inversions. Moderately fractured, but likely intensely fractured near faults, and thus may show fault-controlled propagation anisotropy.

Physical Properties (± 1 SD)

Down-hole geophone survey velocity:

2698 ± 712 m/s (n = 11)

Natural-state bulk density:

1.79 ± 0.22 g/cm^3 (n = 40)

Calculated porosity:

35.6 ± 11.0% (n = 40)

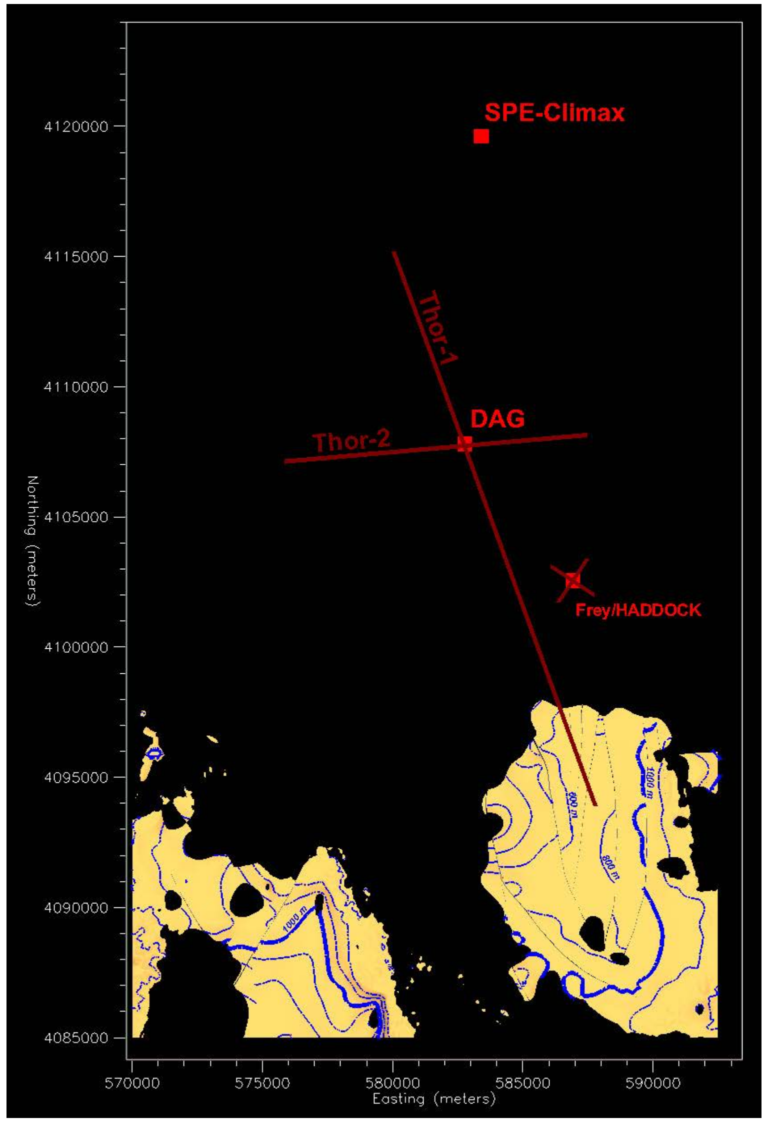

Map view of model area showing extent of LWT.
Blue lines are elevation contours (interval = 200 meters)

Lower Welded Tuff (LWT)

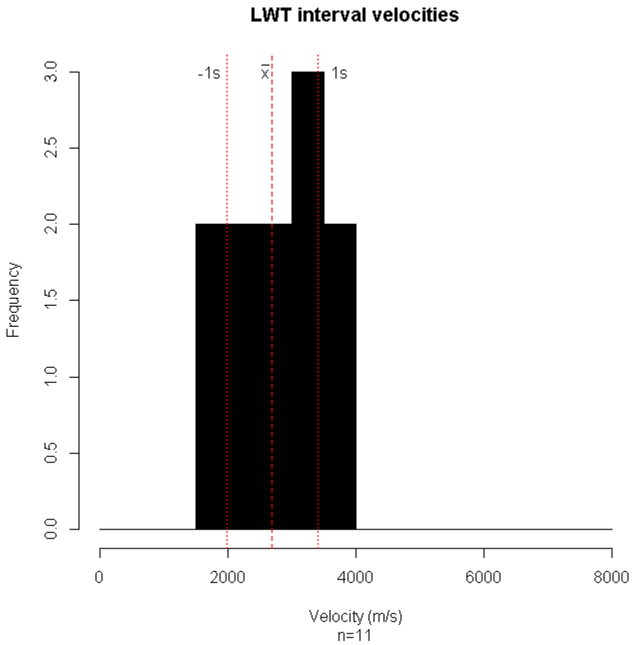

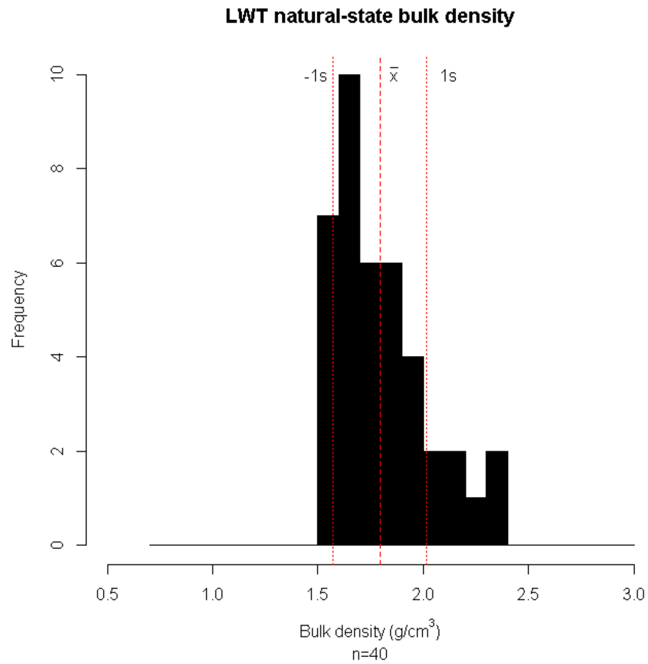

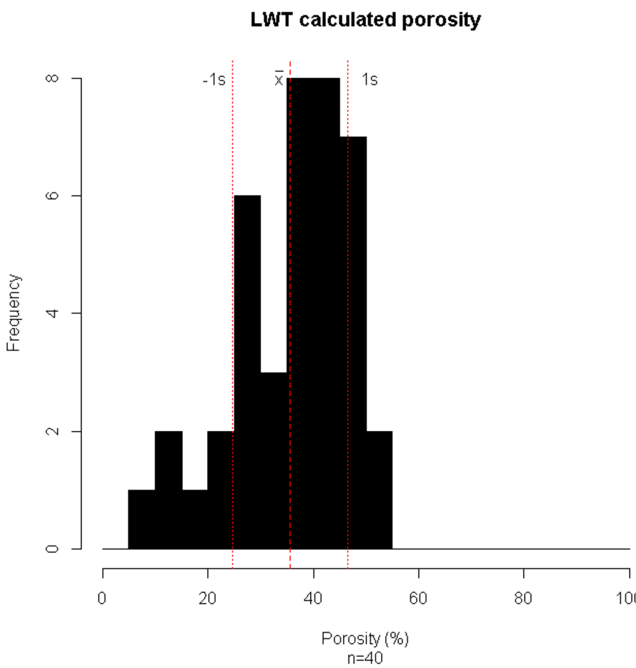

Lower Welded Tuff (LWT)

Photographs

LWT capping hill in Area 19, NNSS.

LWT outcrop, Area 19, NNSS.

Zeolitic Nonwelded Tuff (ZNT)

Stratigraphy

In southern portion of model area, ZNT includes all stratigraphic units from base of welded Topopah Spring Tuff (LWT) to top of Paleozoic sedimentary rocks (PZ). In northern portion of model area where LWT is not present, ZNT includes all stratigraphic units from top of pervasive zeolitization (base of VNT) to top of Paleozoic sedimentary rocks (PZ).

Lithology

Nonwelded to partially welded, zeolitic tuffs. Lithology and alteration become more variable in lower portion.

Structure

Generally poorly fractured but can be moderately fractured in places, particularly near faults.

Seismic Characteristics

Zone of intermediate velocity. Lithologic and alteration variability in lower portion results in more variable physical properties than overlying VNT. Some velocity inversions may be present in lower portion. Basal zone is typically argillic and may have higher velocities. Typically characterized by low reflectivity and energy with poor continuity and coherency. Fracturing around faults may result in fault-controlled propagation anisotropy.

Physical Properties (± 1 SD)

P-wave velocity:

2430 ± 687 m/s (n = 1174)

Natural-state bulk density:

1.83 ± 0.14 g/cm^3 (n = 3270)

Calculated porosity:

39.8 ± 5.9% (n = 3270)

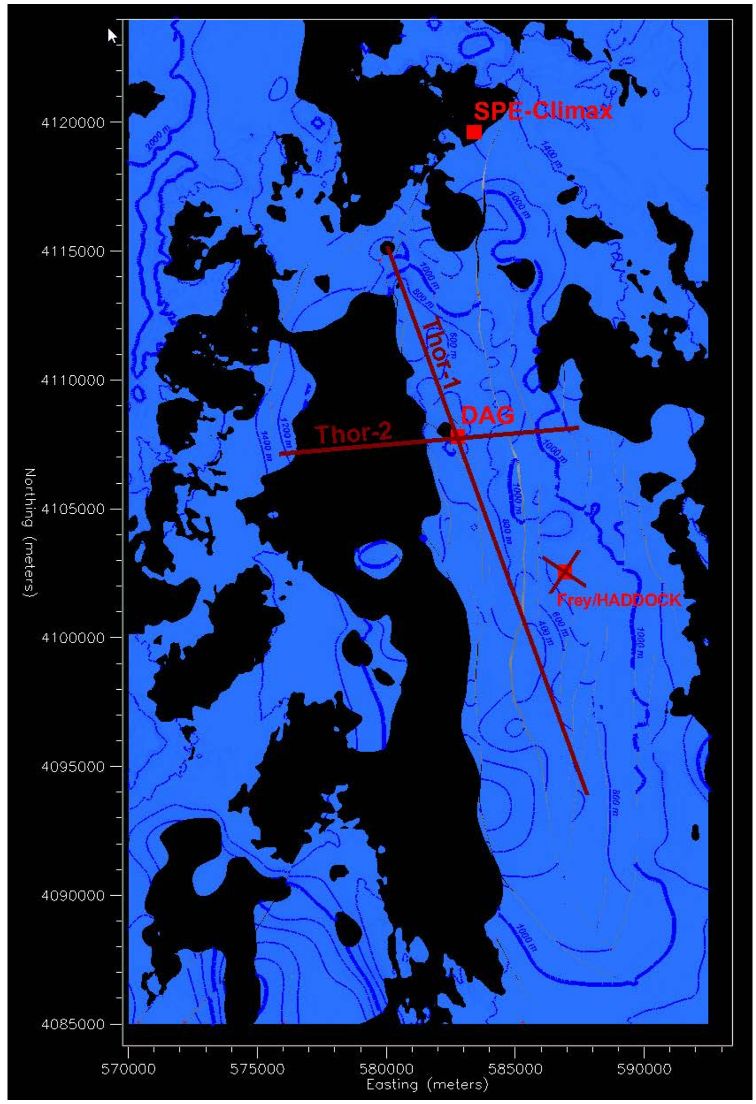

Map view of model area showing extent of ZNT.
Blue lines are elevation contours (interval = 200 meters)

Zeolitic Nonwelded Tuff (ZNT)

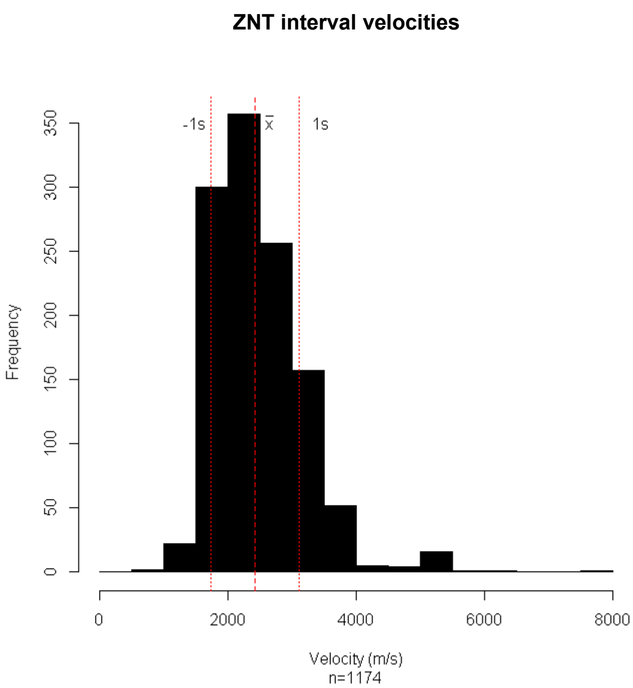

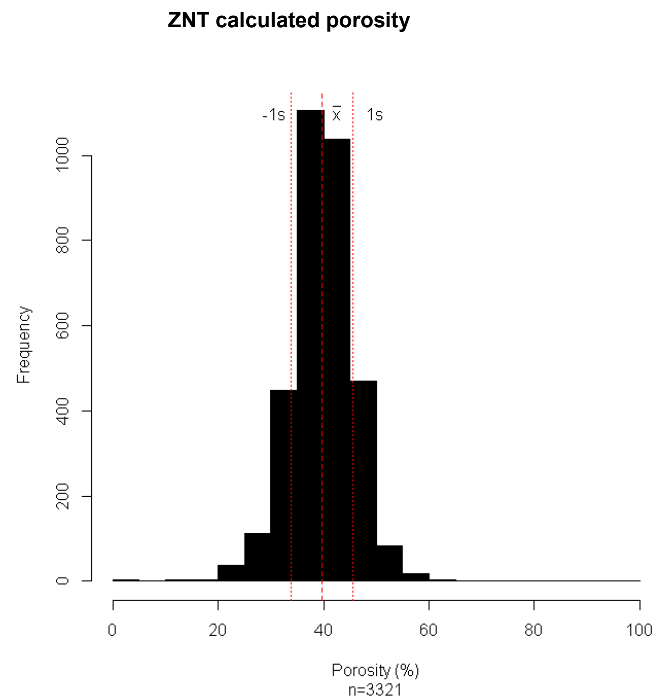

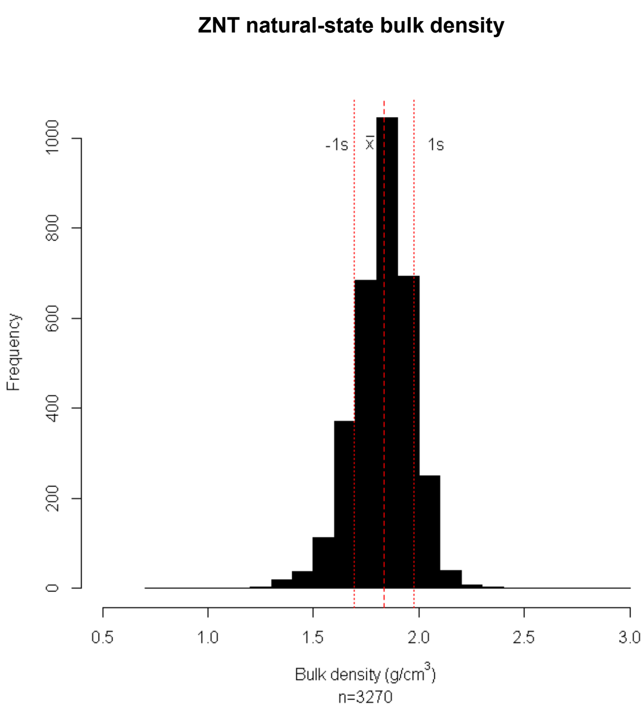

Zeolitic Nonwelded Tuff (ZNT)

Photographs

ZNT outcrop, Area 12, NNSS.

ZNT outcrop, Area 17, NNSS

ZNT outcrop, Area 12, NNSS.

Paleozoic Rocks (PZ)

Stratigraphy

Includes all Precambrian and Paleozoic rocks.

Lithology

Mostly limestone and dolomite, particularly in east half of model area and at depth. Significant occurrences of Precambrian and upper Paleozoic quartzite, siltstone, and shale/argillite occur in northern and western portions of model area.

Structure

Moderately to highly fractured. Complexly deformed with intense folding and thrust faulting, particularly in west half of model area.

Seismic Characteristics

Extensive and very thick high velocity unit. Underlies almost the entire model area. Structural and lithologic differences between the eastern and western portions of model area may result in different seismic character between these areas.

Physical Properties (± 1 SD)

Down-hole geophone survey velocity:

4967 ± 1554 m/s (n = 72)

Natural-state bulk density:

2.45 ± 0.35 g/cm^3 (n = 45)

Calculated porosity:

12.8 ± 13.9% (n = 50)

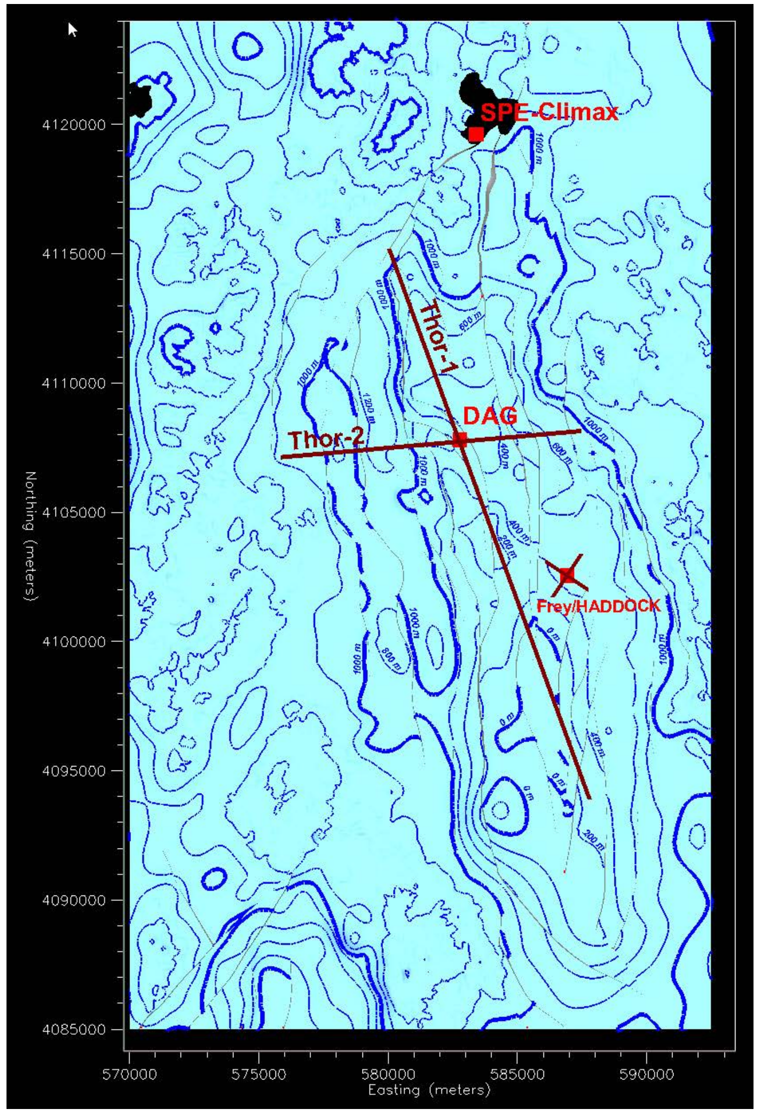

Map view of model area showing extent of Pz.
Blue lines are elevation contours (interval = 200 meters)

Paleozoic Rocks (PZ)

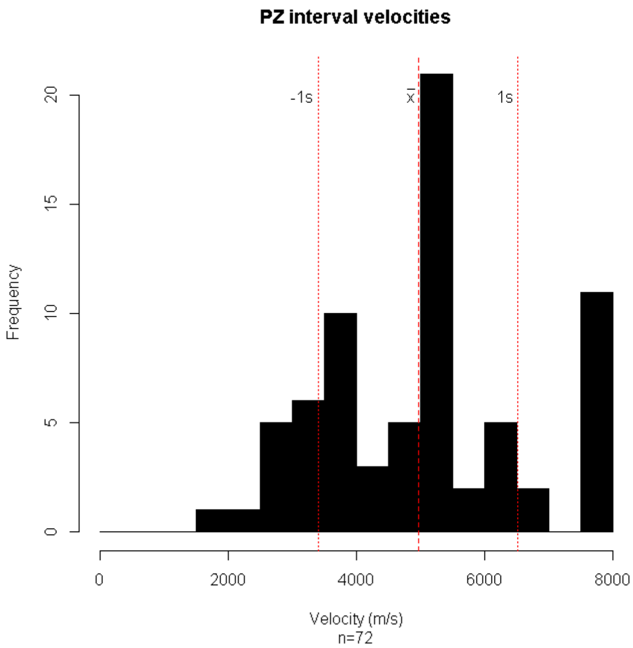

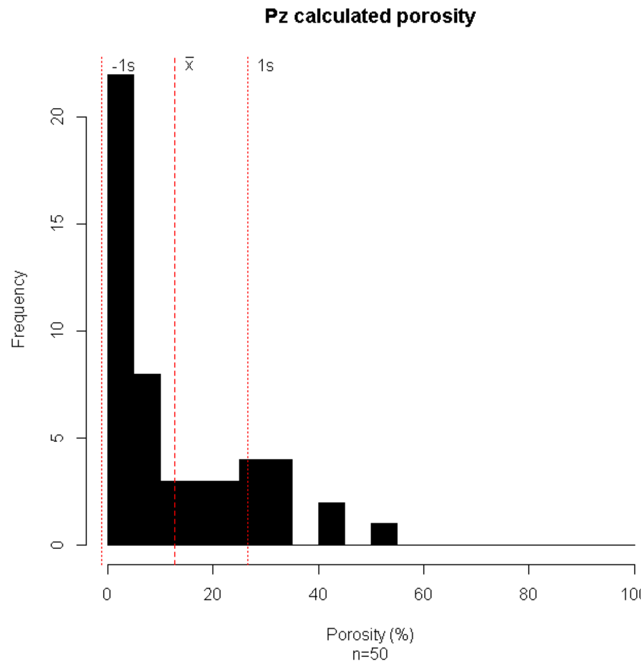

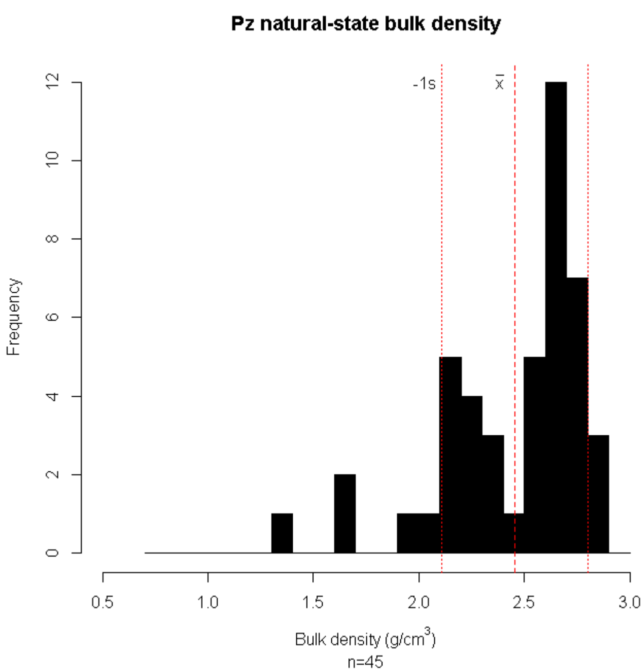

Paleozoic Rocks (PZ)

Photographs

Pz carbonate outcrop, Area 7, NNSS.

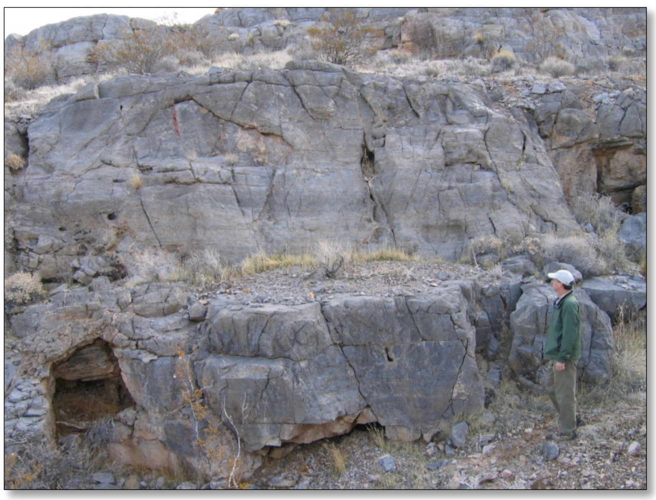

Pz carbonate outcrop, Area 5, NNSS.

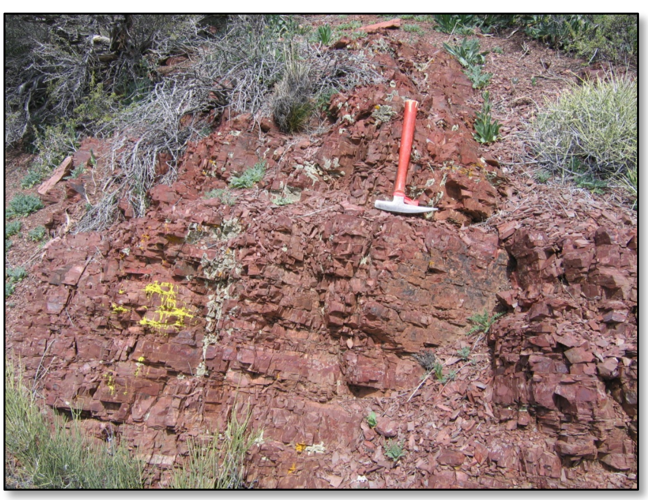

Pz fine-grained siliciclastic outcrop, Area 16, NNSS.

Mesozoic Granite (Mz)

Stratigraphy

Cretaceous granite.

Lithology

Quartz monzonite and granodiorite.

Structure

Moderately to highly fractured. Occur as deep-seated and very steep-sided intrusive igneous stocks.

Seismic Characteristics and Physical Properties

See:

Broome, S. and Pfeifle, T., 2011. Phase 1 Mechanical Property Test Results for Borehole U-15n in Support of NCNS Source Physics Experiment, SAND2011-4394C.

Broome, S. and Lee, M., 2012. Unconfined Compression Mechanical Testing Results on Core from Borehole U-15n#10, Nevada National Security Site, in support of NCNS Source Physics Experiment, SAND2012-9376P.

Broome, S. and Lee, M., 2013. Triaxial compression testing results on core from borehole U- 15n, Nevada National Security Site, in support of NCNS Source Physics Experiment, SAND2013-2913P.

Broome, S. and Lee, M., 2013. Dynamic Brazilian tension results on core from borehole U-15n, Nevada National Security Site, in support of NCNS Source Physics Experiment, SAND2013- 3527P.

Broome, S., Lee, M., and Sussman, A., 2013. Direct Shear and Triaxial Shear test results on core from Boreholes U-15n and U-15n#10, Nevada, in support of Source Physics Experiment, SAND2013-4347P.

Broome, S. and Lee, M., 2014. Unconfined compression test results on core from boreholes U-15n#12 and U-15n#13, Nevada National Security Site, in support of NCNS Source Physics Experiment, SAND2014-16659O.

Hoots, C. R., R. E. Abbott, L. Preston, H. A. Knox, and P. C. Schwering, 2020. Near-Field Imaging of Shallow Chemical Explosions in Granite Using Change Detection Methods with Surface and Borehole Seismic Data, SAND2020-4327.

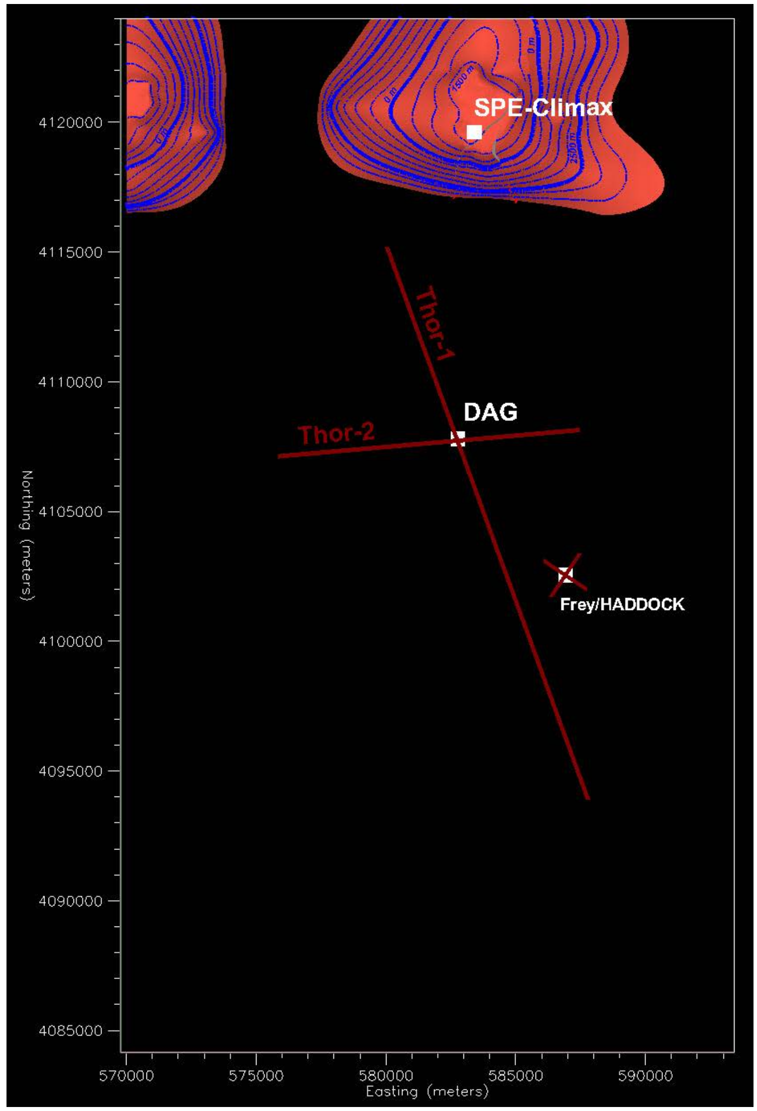

Map view of model area showing extent of Mz.
Blue lines are elevation contours (interval = 500 meters)

Mesozoic Granite (Mz)

Photographs

Mz outcrop, Area 15, NNSS.

Mz outcrop, Area 15, NNSS.